Democratic Republic of Algeria Ministry of Higher Education and Scientific Research

Amar Telidji- Laghouat University

Laboratoire Physique des Matériaux

FACULTY of TECHNOLOGY

MECHANICAL ENGINEERING DEPARTMENT

A dissertation submitted in partial fulfillment for the requirements of the degree of master in mechanical engineering

Presented By :

Mouhssin Abd-Essabour BELACEL

Mohammed Ammar BEN LARBI

DOMAIN: SCIENCES and TECHNOLOGIES

OPTION: ENERGETIC

Theme :

3D Numerical Simulation of Shell and Multipass Tube Heat Exchanger: parametric study

Defense jury:

Member	Quality	Grade
Mr. BENSENOUCI Ahmed	President	MCA
Mr. HAMDI Nassereddine	Reporter	MCB
Mr. HACHANI Lakhdar	Supervisor	Pr

College Year: 2022/2023

Dedications:

To my mom, who have always encouraged and supported me throughout my academic journey. Your unwavering love and belief in me have been my guiding light. and to all my family members. Thank you.

To our advisor Mr. Hachani Lakhdar whose passion for his subjects and dedication to teaching have inspired me. Thank you for pushing me to be my best and for sharing your knowledge with me.

To all my friends.

Ammar

Dedications:

I dedicate this dissertation to my family, who have consistently provided me with the most encouragement and motivation.

I dedicate this work to my parents, who have always supported me in pursuing my goals and who have instilled in me a love of learning and a strong work ethic.

To my sibling, who has served as both my ally and sounding board during this journey.

To our supervisor Pr. Lakhdar HACHANI, who throughout this process has offered us everything, direction, inspiration, and constant support.

To my friend Ammar, who has meticulously been working on this project.

This accomplishment is both yours and mine, so thank you for your love and support.

Mouhssin.

Abstract

This work is mainly based on a full 3D predictive numerical simulation in a stationary regime using Ansys/Fluent CFD software to investigate the heat transfer performances of shell and multipass tube heat exchangers. The focus was on a comparative study between four different cases by changing the heat transfer fluids (oil and water) and their arrangement in terms of flow direction at the inlet and outlet (i.e., same or opposite directions). To accomplish this, we've examined the temperature distribution and fluid flow patterns within the heat exchanger and assessed its efficiency by estimating the heat transfer rate and energy consumption. Finally, we've discussed the ideal configuration in terms of thermal efficiency.

keywords: heat exchanger - shell and multipass tube – CFD software (ANSYS).

Résumé

Ce travail est essentiellement basé sur une simulation 3D numérique prédictive en régime stationnaire en utilisant le logiciel Ansys/Fluent, afin d'examiner les performances thermique d'un échangeur de chaleur de type calandre et multi-passe tubulaire. L'accent a été mis sur une étude comparative entre quatre cas différents en modifiant les fluides caloporteurs (huile et eau) et leur disposition en termes de sens d'écoulement à l'entrée et à la sortie (circulation dans le même sens ou opposées). Pour ce faire, nous avons examiné la répartition de la température et la configuration d'écoulement des fluides dans l'échangeur de chaleur, ainsi que l'évaluation de son efficacité en estimant le taux de transfert de chaleur et la consommation d'énergie. Enfin, nous avons discuté de la configuration idéale en fonction de l'efficacité thermique.

Mots-clés : échangeur de chaleur - calandre et tube multipasse. Ansys/Fluent

ملخص

يعتمد هذا العمل بشكل أساسي على محاكاة رقمية تنبؤية ثلاثية الأبعاد باستخدام برنامج Ansys / Fluent لدراسة والبحث في فعالية الانتقال الحراري لمبادل حراري من نوع الهيكل و أنبوب متعدد الأجزاء. كان التركيز على دراسة مقارنة بين أربع حالات مختلفة عن طريق تغيير سوائل نقل الحرارة (الزيت والماء) وكيفية توزيعها من حيث اتجاه التدفق عند المدخل والمخرج (أي نفس الاتجاه أو الاتجاه المعاكس). لتحقيق ذلك ، قمنا بفحص توزيع درجة الحرارة وأنماط تدفق السوائل داخل المبادل الحراري وقيمنا كفاءته من خلال تقدير معدل نقل الحرارة واستهلاك الطاقة. أخيرًا ، لقد ناقشنا التكوين المثالي من حيث الكفاءة الحرارية.

الكلمات المفتاحية: مبادل حراري - غلاف وأنبوب متعدد الممرات

SUMMARY

LIST OF FIGURES

NOMENCLATURE

SYMBOLES	PARAMETER	UNITE
T	Temperature	°C, °K
$T_{h,in}$	Temperature of hot fluid in the inlet	°C, °K
$T_{h,out}$	Temperature of hot fluid in the outlet	°C, °K
$T_{c,out}$	Temperature of cold fluid in the outlet	°C, °K
$T_{c,in}$	Temperature of cold fluid in the inlet	°C, °K
ΔT_{LM}	Log mean deference temperature	°C, °K
ΔT_s	Temperature drop across the scale	°C, °K
ΔT_{max}	Maximum deference of temperature	°C, °K
Q	Amount of heat	W
$\dot{m}_h$	Mass flow rate for the hot fluid	kg/s
$\dot{m}_c$	Mass flow rate for the cold fluid	kg/s
$\dot{m}$	Mass flow rate	kg/s
m	Mass	kg
cp_h	Specific heat for the hot *fluid*	J/Kg.°C
cp_c	Specific heat for the cold fluid	J/Kg.°C
U	Overall heat transfer coefficient	W/m^2.K
h	Heat transfer coefficient	W/m^2.K
A	Heat transfer surface area	m^2
A_w	Heat transfer area of the wall	m^2
Ac	Cross-sectional flow area.	m^2
R_f	Fouling factor	m^2K/W
R_t	Total thermal resistance	m^2K/W
R_w	Wall thermal resistance	m^2K/W
$Qmax$	Maximum possible heat transfer rate	W
d_i and d_o	Inner and outer diameters of the circular	m
L	Tube length	m
Dh	Hydraulic diameter	m
P_{wetted}	Wetted perimeter	m
δ_w	Thikness of the wall	m
G	Mass velocity	Kg/m^2.S
ρ	Density of the fluid	Kg/m^3
u_m,v	Velocity	m/s
μ	Absolute viscosity	Pa.s
λ_w	Thermal conductivity of the wall	W/m.K

λ	Thermal conductivity	W/m.K
C_{min}	Minimum value of the thermal capacity rate	W/°C
C_{real}	Thermal capacity ratio	W/°C
C_{max}	Maxim value of the thermal capacity rate	W/°C
β	Area density	m^2/m^3
E	Total energy per unit mass	J/kg
W	Work done on the system	J
e	Internal energy per unit mass	J
P_k	Turbulence production terme	W/m^3
ϵ	Dissipation rate of turbulent kinetic energy	W/kg
μ_{eff}	Effective viscosity	Pa.s
μ_t	Turbulent viscosity	Pa.s

List of tables:

Dimensionless groups

Re	Reynolds number
Nu	Nusselt number
pr	Prandtl number
ε	The heat exchanger effectiveness
Cr	The heat capacity ratio

General introduction

Heat exchangers are important components in industrial processes as they facilitate the transfer of thermal energy between fluids. They come in different types, sizes, and shapes and are categorized based on factors like their design, operating principles, and types of heat transfer mechanisms involved, [7].

The purpose of this research is to use Computational Fluid Dynamics (CFD) software, specifically ANSYS, to numerically analyze the thermal and dynamic behaviors of a heat exchanger shell and multipass tube type in a stationary regime, and to identify the dominant factors influencing heat transfer within the system. Moreover, this study includes a comparison between two configurations with different cooling fluids (oil and water) and in the same or opposite directions.

This dissertation is composed of three chapters. The first chapter provides a comprehensive classification overview of heat exchangers, including direct and indirect transfer types, shell-and-tube exchangers, plate exchangers, and more. This chapter also introduces the LMT method, which calculates the log mean temperature difference between hot and cold fluids within a heat exchanger, and discusses the assumptions, limitations, and procedures for its implementation. Additionally, the chapter covers factors affecting the LMT and offers guidelines for selecting appropriate values for correction factors used in the LMT method. Furthermore, the overall heat transfer coefficient and its conjunction with the LMT method in computing the heat transfer rate are discussed. The ε-NTU method and its practical application in designing and analyzing heat exchangers are also explained.

The second chapter statistically explores the heat transfer performances that occur in a shell and multipass heat exchanger, with an emphasis on thermal and dynamic evolutions. This is accomplished by inspecting the temperature distribution and fluid flow patterns in the device, as well as assessing the performance of the heat exchanger by calculating the heat transfer rate between the two fluids and the energy required to operate the device.

Furthermore, the most important steps in terms of geometry construction, the different functions used for mesh adaptation, and the setup stage of the calculation, as well as the necessary equations used in modeling the phenomena, are discussed in detail in this chapter.

The third chapter focuses on the discussion and comparative analysis of numerical results obtained from four different cases of shell and multipass tube heat exchangers. These cases involve water-water and oil-water with both opposite and the same inlets. The objective of this analysis is to evaluate the overall heat transfer characteristics of each type of heat exchanger in terms of temperature field, dynamic field, and thermal efficiency. The analysis considers various performance metrics, such as the heat transfer coefficient and overall heat transfer rate, and the results are presented and compared through visualizations, including contours, charts, and streamlines. The findings of this study can provide valuable insights into the design and operation of shell and multipass tube heat exchangers, helping engineers to optimize their performance for specific applications.

CHAPTER I

GENERALITY OF HEAT EXCHANGER

Introduction

Heat exchangers play a crucial role in various industrial processes by facilitating the transfer of thermal energy between fluids. They can take on different shapes and sizes and are classified based on their design, operating principles, and the type of heat transfer involved. In this chapter, we will provide a comprehensive overview of heat exchanger classification, including different classification systems such as direct and indirect transfer types, shell-and-tube exchangers, plate exchangers, and more.

Additionally, we will introduce the LMT method, which is utilized in calculating the log mean temperature difference between hot and cold fluids within a heat exchanger. We will cover the assumptions and limitations of the LMT method and provide step-by-step procedures for its implementation across various types of heat exchangers also discuss the factors that affect the LMT and provide guidelines for selecting appropriate values for the correction factors used in the LMT method. Furthermore, we will discuss the overall heat transfer coefficient and its conjunction with the LMT method in computing the heat transfer rate in a heat exchanger.

Moreover, we will the ε-NTU method and its practical application in designing and analyzing heat exchangers. we will explain how the ε-NTU method is utilized to calculate the thermal effectiveness of a heat exchanger.

By the end of this chapter, you will have a solid understanding of the classification of the heat exchanger also the LMT method, and its practical application, also you can learn how to calculate with the ε-NTU method.

CHAPTER I

PART I: CLASSIFICATION OF HEAT EXCHANGERS

This part was inspired directly from the first edition of Fundamentals of Heat Exchanger Design book, published by Ramesh K. Shah, Dušan P. Sekulić , (2003) John Wiley & Sons, USA, which is based on the classification of heat exchangers and their thermal performances.

1. Classification according to transfer processes

Heat exchangers are classified according to transfer processes into indirect and direct contact types.

1.1. Indirect-contact heat exchangers

In an indirect-contact heat exchanger, the fluid streams remain separate and the heat transfers continuously through an impervious dividing wall or into and out of a wall in a transient manner. Thus, ideally, there is no direct contact between thermally interacting fluids. This type of heat exchanger also referred to as a surface heat exchanger, can be further classified into direct-transfer type, storage type, and fluidized-bed exchangers, [2].

This can be further divided into:

1.1.1. Direct transfer type (recuperate)

Those exchangers in which the heat transfer between fluids takes place directly through a separating wall (e.g., tube/pipe wall) are called a direct transfer type or simply a recuperate. Here the fluids do not mix with each other, there is a continuous flow of heat from hot fluid to cold fluid and there are no moving parts, [1].

1.1.2. Storage type

Also called a fixed matrix or fixed bed regenerator this is a periodic flow heat transfer device. This makes use of a matrix that has a high thermal capacity, through which hot and cold fluid pass alternatively.

At least two matrices are required. As shown below in Figure I.1 initially matrix A is heated by hot fluid and matrix B is cooled by the cold fluid. After a certain interval of time, the valves are operated such that hot fluid flows through previously cooled matrix B and gets cooled by transferring heat to it. Similarly, cold fluid passes through matrix A which was previously heated, the cold fluid takes heat from it to become heated.

Figure I.1: Storage type exchanger, [1].

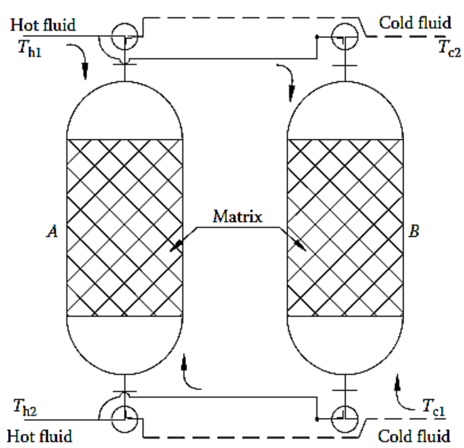

In recuperators, fundamental loss occurs only through the wall during heat conduction, but in Storage type regenerators as we are using intermediate thermal storage there is a bigger heat loss during the heat in and out from the intermediate storage, [1].

1.1.3. Fluidized bed type

In other cases, and as depicted in Figure I.2 the hot air passes through the bottom of the exchanger tower. There is a finely divided solid material at the bottom of the exchanger. When the upward fluid velocity is low, the solid particles will remain fixed and the fluid will pass through the interstices of the bed. But when the fluid velocity is high the solid particles will be carried away with the fluid. When the upwards drag force on the particles is higher than the weight of the solid particle the solid particles float inside the whole bed volume. This solid particle mixed with gas floating throughout the tower behaves like a liquid. This characteristic is referred to as a fluidized bed condition, [1].

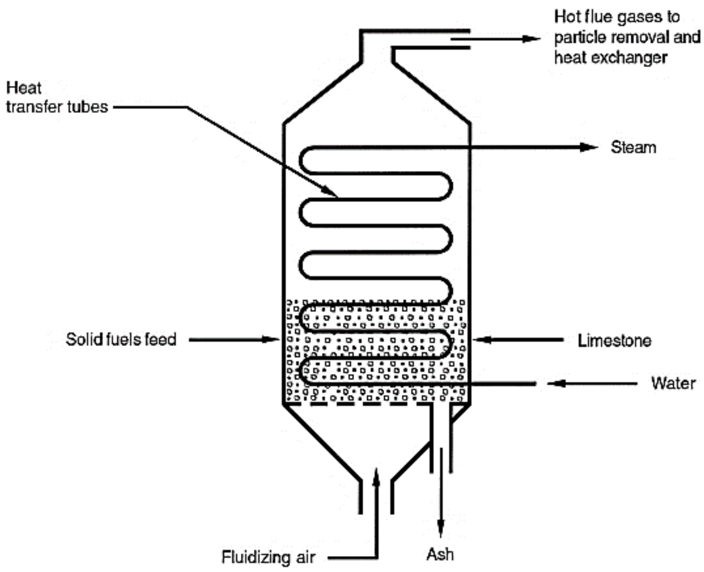

Figure I.2: Fluidized bed heat exchanger, [1].

A very high heat transfer coefficient is achieved on the fluidized bed. A fluidized bed heat transfer mechanism is used in chemical reactor engineering, drying, mixing, and absorption processes.

1.2. Direct-contact heat exchangers

In a direct-contact exchanger, two fluid streams come into direct contact, exchange heat, and are then separated. Common applications of a direct-contact exchanger involve a mass transfer in addition to heat transfer, such as in evaporative cooling and rectification; applications involving only sensible heat transfer are rare. The enthalpy of phase change in such an exchanger generally represents a significant portion of the total energy transfer. The phase change generally enhances the heat transfer rate, [2].

Compared to indirect-contact recuperates and regenerators, in direct-contact heat exchangers,

- very high heat transfer rates are achievable,
- The exchanger construction is relatively inexpensive,
- The fouling problem is generally non-existent, due to the absence of a heat transfer surface (wall) between the two fluids.

However, the applications are limited to those cases where direct contact with two fluid streams is permissible. The design theory for these exchangers is beyond the scope of this book and is not covered. These exchangers may be further classified as follows, [1].

1.2.1. Immiscible fluid exchangers

In this type, two immiscible fluid streams are brought into direct contact. These fluids may be single-phase fluids or they may involve condensation or vaporization. Condensation of organic vapors and oil vapors with water or air are typical examples, [1].

1.2.2. Gas-liquid exchangers

In this type, one fluid is a gas (more commonly, air) and the other a low-pressure liquid (more commonly, water) and is readily separable after the energy exchange. In either cooling of liquid (water) or humidification of gas (air) applications, liquid partially evaporates and the vapor is carried away with the gas. In these exchanges, more than 90% of the energy transfer is by virtue of mass transfer (due to the evaporation of the liquid), and convective heat transfer is a minor mechanism. A ‘‘wet’’ (water) cooling tower with forced-or natural-draft airflow is the most common application. Other applications are the air-conditioning spray chamber, spray drier, spray tower, and spray pond, [1].

1.2.3. Liquid–vapor exchangers

In this type, typically steam is partially or fully condensed using cooling water, or water is heated with waste steam through direct contact in the exchanger. No condensable and residual steam and hot water are the outlet streams. Common examples are desuperheaters and open-feed water heaters (also known as deaerators) in power plants, [1].

2. Classification according to flow arrangement:

The basic flow arrangement of the fluids in a heat exchanger is as follows:

Parallel-flow, Counter-flow, Cross-flow

The choice of a particular flow arrangement is dependent upon the required exchanger effectiveness, fluid flow paths, packaging envelope, allowable thermal stresses, temperature levels, and other design criteria, [3]. These basic flow arrangements are discussed next.

2.1. Parallel-flow: Here both fluids enter at the same end, flow parallel to each other in the same direction, and leave at the other end.

2.2. Counter-flow: Here both fluids flow parallel to each other but in opposite directions.

This is the most efficient flow arrangement among others in single pass arrangement with the same parameter.

2.3. Cross-flow: Here both fluids flow parallel and perpendicular to each other.

The above flow arrangements are depicted below in the figure i.3:

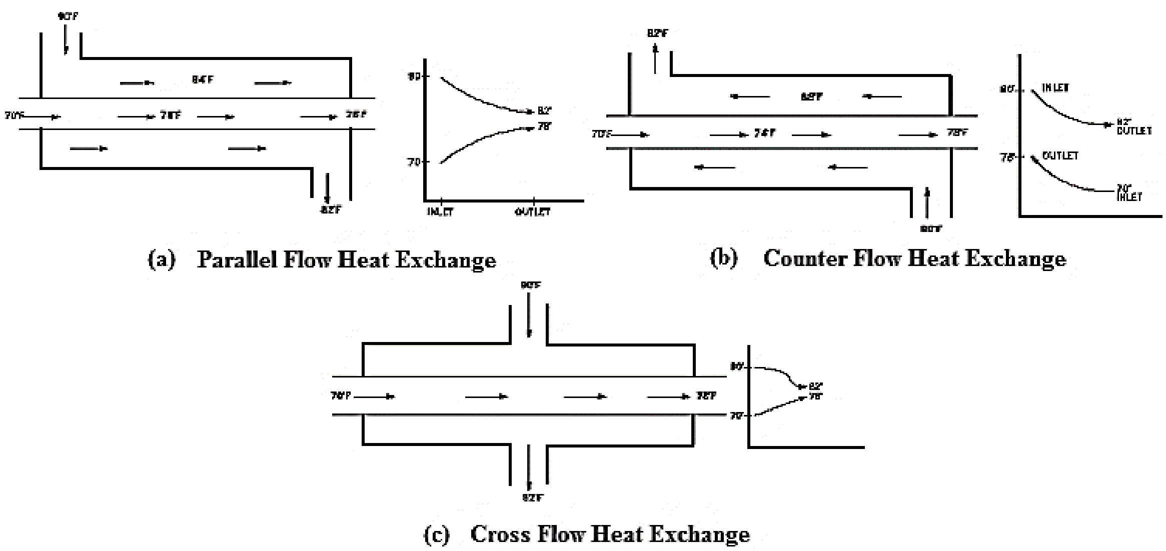

Figure I.3: Type of heat exchanger: parallel-flow, counter-flow, cross-flow.

3. Classification according to pass arrangement:

These are either single-pass or multipass. A fluid is considered to have made one pass if it flows through a section of the heat exchanger through its full length once. In a multipass arrangement. a fluid is reversed and flows through the flow length two or more times, [3].

3.1. Single pass: Here the fluid flows through the heat exchanger along its length once.

3.2. Multi pass: Here the fluid flows through the heat exchanger along its length and then it's reversed to flow again through the whole length again. In multipass arrangements, the flow can pass along the length of the heat exchanger 2 or more times. multipass arrangements are used when the design of the heat exchanger results in extreme length, significantly low velocities, or low effectiveness, [3].

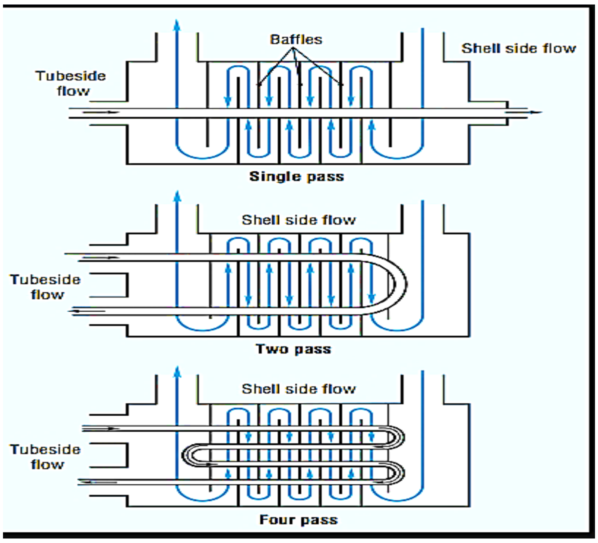

Figure I.4: Single-pass vs multipass heat exchanger flow, [3].

4. Classification according to the number of fluids:

Most processes of heating, cooling, heat recovery and heat rejection involve the transfer of heat between two fluids. Hence, two-fluid heat exchangers are the most common. Three-fluid heat exchangers are widely used in cryogenics and some chemical processes (e.g., air separation systems, a helium–air separation unit, purification and liquefaction of hydrogen, and ammonia gas synthesis). Heat exchangers with as many as 12 fluid streams have been used in some chemical process applications, [1].

5. Classification according to surface compactness:

Compact heat exchangers are important when there are restrictions on the size and weight of exchangers. A compact heat exchanger incorporates a heat-transfer surface having a high area density β, somewhat arbitrarily 700 m^2/m^3 (200 ft^2/ft^3) and higher. The area density β is the ratio of heat transfer area A to its volume V. A compact heat exchanger employs a compact surface on one or more sides of a two-fluid or a multifluid heat exchanger. They can often achieve higher thermal effectiveness than shell and tube exchangers (95% vs. the 60-80% typical for shell and tube heat exchangers), which makes them particularly useful in energy-intensive industries, [6]. For the least capital cost, the size of the unit should be minimal. There are additional advantages to small volumes. Some of these are:

- Small inventory, making them good for handling expensive or hazardous materials, [6]
- Low weight
- Easier transport
- Less foundation
- Better temperature control

Some barriers to the use of compact heat exchangers include, [6]:

- The lack of standards similar to pressure vessel codes and standards, although this is now being redressed in the areas of plate-fin exchangers and air-cooled exchangers.
- Narrow passages in plate-fin exchangers make them susceptible to fouling and cannot be cleaned mechanically.

This limits their use to clean applications like handling air, light hydrocarbons, and refrigerants, [2].

6. Classification according to construction features:

Heat exchangers are frequently characterized by construction features. Four major construction types are tubular, plate-type, extended surface, and regenerative exchangers. Heat exchangers with other constructions are also available, such as scraped surface exchangers, tank heaters, cooler cartridge exchangers, and others (Walker, 1990). Some of these may be classified as tubular exchangers, but they have some unique features compared to conventional tubular exchangers. Since the applications of these exchangers, [1].

6.1. Tubular heat exchangers:

These exchangers are generally built of circular tubes, although elliptical, rectangular, or round/flat twisted tubes have also been used in some applications. There is considerable flexibility in the design because the core geometry can be varied easily by changing the tube diameter, length, and arrangement. Tubular exchangers can be designed for high pressures relative to the environment and high-pressure differences between the fluids. Tubular exchangers are used primarily for liquid -to liquid and liquid-to-phase change (condensing or evaporating) heat transfer applications. They are used for gas-to-liquid and gas-to-gas heat transfer applications primarily when the operating temperature and/ or pressure is very high or fouling is a severe problem on at least one fluid side and no other types of exchangers would work. These exchangers may be classified as shell-and-tube, double-pipe, and spiral-tube exchangers. They are all prime surface exchangers except for exchangers having fins outside/inside tubes, [1].

6.2. Shell-and-tube exchangers:

This exchanger is generally built of a bundle of round tubes mounted in a cylindrical shell with the tube axis parallel to that of the shell. One fluid flow inside the tubes and the other flows across and along the tubes. The major components of this exchanger are tubes (or tube bundle), shell, front-end head, rear-end head, baffles, and tube sheets, and are described in many books on Heat Transfer A variety of different internal constructions are used in shell-and-tube exchangers, depending on the desired heat transfer and pressure drop performance and the methods employed to reduce thermal stresses, to prevent leakages, to provide for ease of cleaning, to contain operating pressures and temperatures, to control corrosion, to accommodate highly asymmetric flows, and so on

Shell -and-tube exchangers are classified and constructed in accordance with the widely used TEMA (Tubular Exchanger Manufacturers Association) standards (TEMA, 77/1999), HE-I81, DIN, and other standards in Europe and elsewhere, and ASME (American Society of Mechanical Engineers) boiler and pressure vessel codes. TEMA has developed a notation system to designate major types of shell-and-tube exchangers. In this system, each exchanger is designated by a three-letter combination, the first letter indicating the front-end head type, the second the shell type, and the third the rear-end head type. Some common shell-and-tube exchangers are AES, BEM, AEP, CFU, AKT, and AJW. It should be emphasized that there are other special types of shell-and-tube exchangers commercially available that have front-and rear-end heads Those exchangers may not be identifiable by the TEMA letter designation.

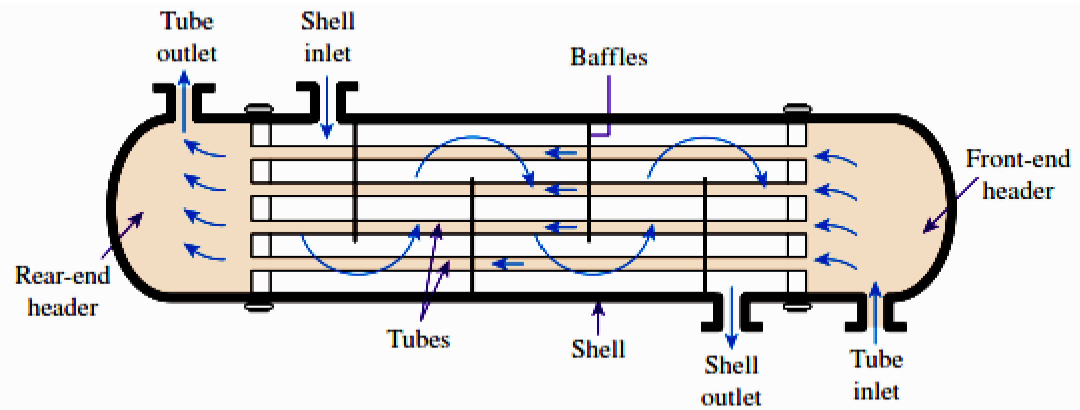

Figure I.5: (a) Shell-and-tube exchanger (BEM) with one shell pass and one tube pass; [1].

The three most common types of shell-and-tube exchangers are:

- fixed tube sheet design.
- U-tube design.
- floating-head type.

In all three types, the front-end head is stationary while the rear-end head can be either stationary or floating depending on the thermal stresses in the shell, tube, or tube sheet, due to temperature differences as a result of heat transfer. The exchangers are built in accordance with three mechanical standards that specify the design, fabrication, and materials of unfired shell-and-tube heat exchangers. Class R is for the generally severe requirements of petroleum and related processing applications. Class C is for generally moderate requirements for commercial and general process applications. Class B is for chemical process service. The exchangers are built to comply with the applicable ASME Boiler and Pressure Vessel Code, Section VIII, IS 2825, IS 4506, and other pertinent codes and/or standards. The TEMA standards supplement and define the ASME code for heat exchanger applications. In addition, state and local codes applicable to the plant location must also be met. The TEMA standards specify the manufacturing tolerances for various mechanical classes, the range of tube sizes and pitches, baffling and support plates, pressure classification, tube sheet thickness formulas, and so on, and must be consulted for all these details. In this book, we consider only the TEMA standards where appropriate, but there are other standards, such as DIN 28 008. Tubular exchangers are widely used in industry for the following reasons. They are custom designed for virtually any capacity and operating conditions, such as from high vacuum to ultrahigh-pressure [over 100 MPa (15,000 psi)], from cryogenics to high temperatures [about 11008 °C (20008 °F)] and any temperature and pressure differences between the fluids, limited only by the materials of construction. They can be designed for special operating conditions: vibration, heavy fouling, highly viscous fluids, erosion, corrosion, toxicity, radioactivity, multi-component mixtures, and so on. They are the most versatile exchangers, made from a variety of metal and nonmetal materials (such as graphite, glass, and Teflon) and range in size from small 0.1 m 2 to supergiant, [1].

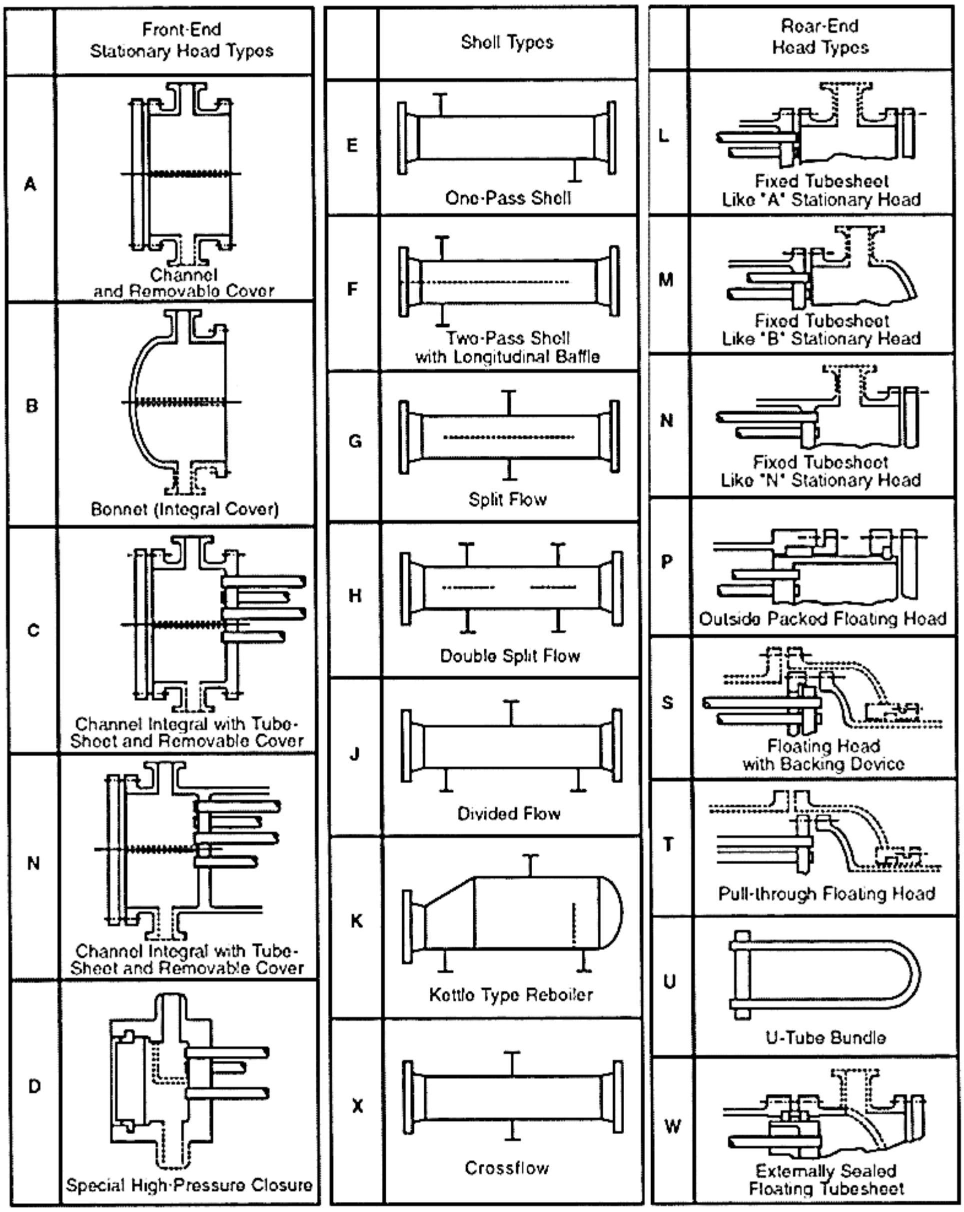

Figure I.6: Standard shell types and front- and rear-end head types (From TEMA, 1999), [1].

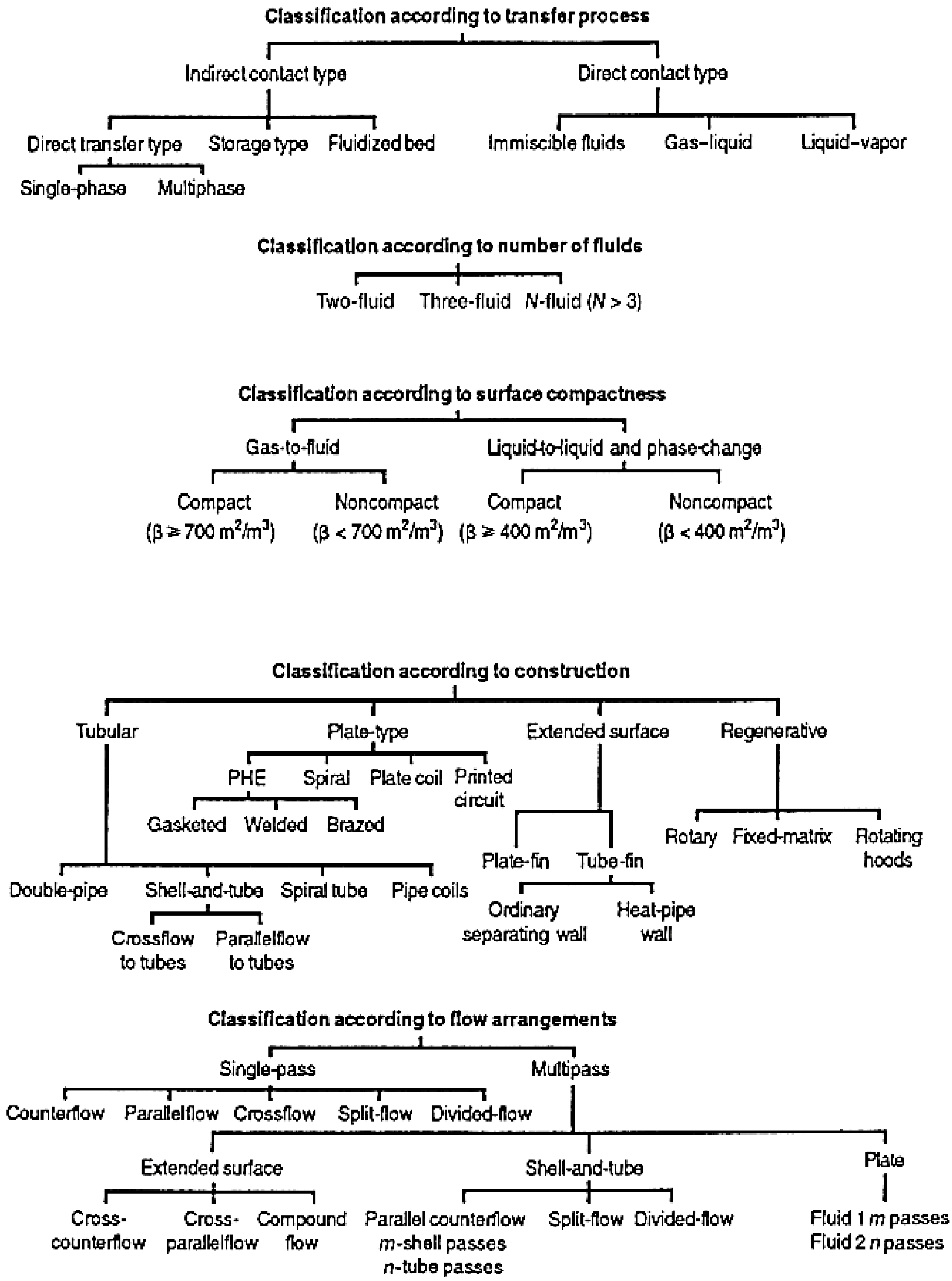

Figure I.7: Classification of heat exchangers.

CHAPTER I

PART II. Theoretical Calculation

The theoretical development performed in this part was mainly inspired from the 5th Edition of Heat and Mass Transfer: Fundamentals and Applications book, published by Yunus A. Çengel, Afshin J. Ghajar, (2015), McGraw-Hill Education, USA.

1. Counter-flow and parallel-flows:

As shown in Fig. I.8, both flow configurations are considered, namely Counter-flow and Parallel-Flows. We have hot and cold fluids and the subscripts (in) and (out) indicate inlet and outlet, respectively. The mass flow rate is expressed as $\dot{m}$.

Counter-flow:

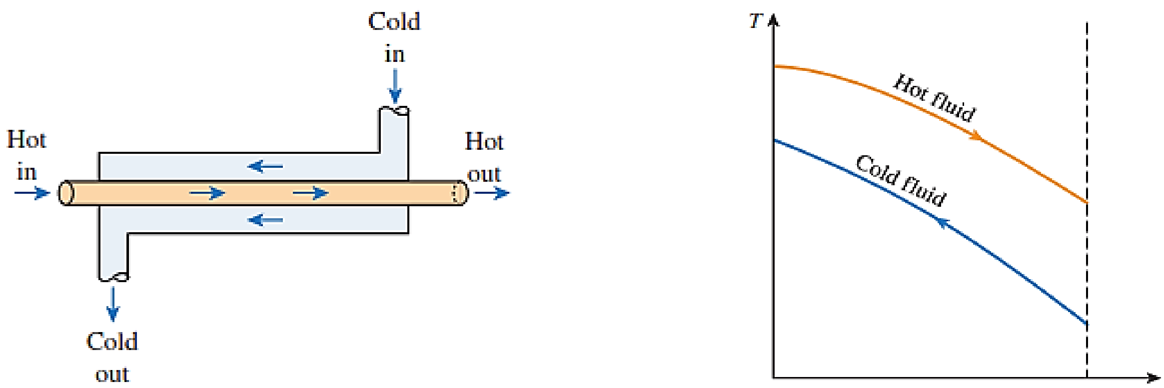

Parallel-Flow:

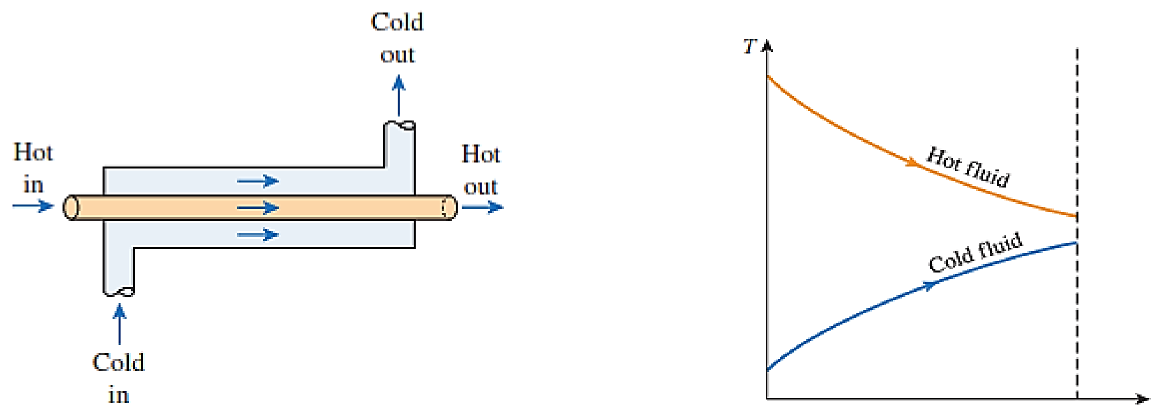

Figure I.8: Counter-flow and parallel-flows.

For the hot fluid, the heat transfer rate is:

$$Q = \dot{m}_h cp_h (T_{h,in} - T_{h,out}) \qquad \textbf{(I.1)}$$

Where $\dot{m}_h$ is the mass flow rate for the hot fluid and cp_h is the specific heat for the hot fluid.

For the cold fluid, the same heat transfer is expressed as, [3]:

$$Q = \dot{m}_c cp_c (T_{c,out} - T_{c,in}) \qquad \textbf{(I.2)}$$

Where $\dot{m}_c$ is the mass flow is the rate for the cold fluid and cp_c is the specific heat for the cold fluid.

The same heat transfer rate can be expressed in terms of the overall heat transfer coefficient:

$$Q = UAF\Delta T_{LM} \tag{I.3}$$

Where U is the overall heat transfer coefficient and A is the heat transfer surface area at the hot or cold side. F is the correction factor, depending on the flow arrangements. For example, F = 1 for counter-flow or parallel-flow such as the double-pipe heat exchangers, and usually F ≤ 1 for other types of flow arrangements.

Note that:

$$UA = U_1A_1 = U_2A_2 \tag{I.4}$$

And ΔT_{LM} is the log mean temperature difference that is defined as:

$$\Delta T_1 = T_{h,in} - T_{c,in} \text{ and } \Delta T_2 = T_{h,out} - T_{c,out} \quad \text{parallel-flow} \tag{I.5}$$

$$\Delta T_1 = T_{h,in} - T_{c,out} \text{ and } \Delta T_2 = T_{h,out} - T_{c,in} \quad \text{counter-flow} \tag{I.6}$$

Equations (I.1), (I.2), and (I.3) are the basic equations for counter-flow and parallel-flow heat exchangers. Hence, any combinations of three unknowns among all parameters (T_1, T_2, A_0, U) can be solved where the heat transfer area is:

$$A_1 = P_1L \tag{I.7}$$

Or:

$$A_2 = P_2L \tag{I.7a}$$

Where $P_1$and P_2 are perimeters of hot and cold fluid channels, respectively.

- ***Overall heat transfer coefficient U:***

Most heat exchanger surfaces tend to acquire an additional heat transfer resistance that increases with time.

This may either be a very thin layer of oxidation or, at the other extreme, it may be a thick crust deposit, such as that which results from a salt-water coolant in steam condensers. This fouling effect can be taken into consideration by introducing an additional thermal resistance, termed the fouling resistance Rs. Its value depends on the type of fluid, fluid velocity, type of surface, and length of service of the heat exchanger. In addition, fins are often added to the surfaces exposed to either or both fluids, and by increasing the surface area, they reduce the resistance to convection heat transfer. The overall heat transfer coefficient for a single smooth and clean plane wall can be calculated from, [4]:

$$UA = \frac{1}{R_t} = \frac{1}{\frac{1}{h_i A} + \frac{\delta_w}{\lambda A} + \frac{1}{h_o A}} \quad \textbf{(I.8)}$$

where R_t is the total thermal resistance to heat flow across the surface between the inside and outside flow, δ_w is the thickness of the wall, and h_i and h_O are heat transfer coefficients for inside and outside flows, respectively. For the unfinned and clean tubular heat exchanger, the overall heat transfer coefficient is given by, [4]

$$U_o A_o = U_i A_i = \frac{1}{R_t} = \frac{1}{\frac{1}{h_i A_i} + \frac{ln\left(\frac{r_o}{r_i}\right)}{2\pi\lambda L} + \frac{1}{h_o A_o}} \quad \textbf{(I.9)}$$

where the area A is the original heat transfer area of the surface before scaling and ΔT_s is the temperature drop across the scale. $R_f = 1/h_s$ is termed the fouling factor (i.e., unit fouling resistance), which has the unit of m^2K/W, [4].

This is discussed in detail in the following chapters, and tables are provided for the values of R_f.

We now consider heat transfer across a heat exchanger wall fouled by deposit formation on both the inside and outside surfaces. The total thermal resistance R_t can be expressed as, [4].

$$R_t = \frac{1}{\mathrm{UA}} = \frac{1}{\mathrm{U_o A_a}} = \frac{1}{U_i A_i} = \frac{1}{h_i A_i} + R_w + \frac{R_{fi}}{A_i} + \frac{R_{fo}}{A_o} + \frac{1}{A_o h_o} \quad \textbf{(I.10)}$$

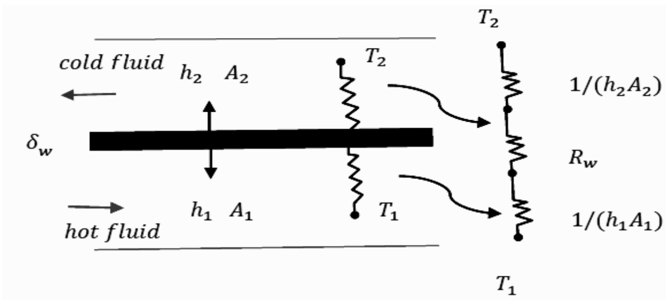

Figure I.9 Thermal resistance and thermal circuit for a heat exchanger

The calculation of an overall heat transfer coefficient depends upon whether it is based on the cold- or hot-side surface area, since $U_o \neq U_i$ if $A_o \neq A_i$. The wall resistance R_w is obtained from the following equations, [4]:

For flat walls, the wall thermal resistance is:

$$R_w = \frac{\delta_w}{k_w A_w} \quad \textbf{(I.11)}$$

Where δ_w is the thickness of the flat wall and λ_w is the thermal conductivity of the wall and A_w is the heat transfer area of the wall, which is the same as A_1 or A_2 in this case for concentric tubes (double-pipe heat exchanger), the wall thermal resistance is:

$$R_w = \frac{ln\left(\frac{d_o}{d_i}\right)}{2\pi\lambda wL} \qquad (I.12)$$

Where d_i and d_o are the inner and outer diameters of the circular wall and L is the tube length.
The overall heat transfer coefficient for the cold fluid with the heat transfer area A_2 is:

$$U_2 = \frac{\frac{1}{A_2}}{\frac{1}{h_1A_1}+R_{wall}+\frac{1}{h_2A_2}} \qquad (I.13)$$

For a double-pipe heat exchanger (concentric pipes) with neglecting the wall conduction we have:

$$U_0 = \frac{1}{\frac{d_o}{h_id_i}+\frac{1}{h_o}} \qquad (I.13a)$$

- ***Flow properties:***

The noncircular diameters in the flow channels are approximated using the hydraulic diameter D_h for the Reynolds number and the equivalent diameter D_h for the Nusselt number.
The hydraulic diameter is defined as*:*

$$D_h = \frac{4A_c}{P_{wetted}} = \frac{4A_cL}{P_{wetted}\,L} = \frac{4A_cL}{A_t} \qquad (I.14)$$

Where P_{wetted} is the wetted perimeter A_c the total heat transfer area and L the length of the channel.

The mass velocity G is defined as:

$$G = \rho u_m \qquad (I.15)$$

The mass flow rate ṁ is defined as:

$$\dot{m} = \rho u_m A_c = GA_c \qquad (I.16)$$

Then, the Reynolds number is expressed as:

$$ReD = \frac{\rho u_m D_h}{\mu} = \frac{mD_h}{A_c\mu} = \frac{GD_h}{\mu} \qquad (I.17)$$

where ρ is the density of the fluid and u_m is the mean velocity of the fluid and D_h is the hydraulic diameter and μ is the absolute viscosity and A_c are the cross-sectional flow area.

- ***Nusselt number:***

The Nusselt number correlations again depend on the flow regime divided into three (Soni et al., 2009), [5]:

$$\boldsymbol{Nu = f(Re, Pr, D_h, L, \mu)} \tag{I.18}$$

With

$$\boldsymbol{Nu = \frac{h_f D_h}{\lambda}} \tag{I.18a}$$

$$\boldsymbol{Pr = \frac{\mu C_p}{\lambda}} \tag{I.18b}$$

where h_f is the heat transfer coefficient (w/m².K); λ is the thermal conductivity (w/m.K); C_p is specific heat (J/kg K); subscript f denotes the fluid phase; D_h is the hydraulic diameter, [5].

Re < 2100 laminar regime:

$$\boldsymbol{Nu = 1.86\left(Re\,Pr\frac{D_h}{L}\right)^{0.33}\left(\frac{\mu_{bf}}{\mu_{wf}}\right)^{0.14}} \tag{I.19}$$

2100 < Re < 10000 transitional regimes:

$$\boldsymbol{Nu = 0.023Re^{\frac{2}{3}}Pr^{0.33}\left(\frac{\mu_{bf}}{\mu_{wf}}\right)^{0.14}} \tag{I.20}$$

Geankoplis (1993) recommends the following correlation for turbulent flow regime:

$$\boldsymbol{Nu = 0.027Re^{0.8}Pr^{C}\left(\frac{\mu_{bf}}{\mu_{wf}}\right)^{0.14}} \tag{I.21}$$

where c is 0.45 in case of heating and 0.35 for cooling.

The heat transfer coefficient for the membrane can be calculated as:

$$\boldsymbol{h = \frac{\lambda}{\delta}} \tag{I.22}$$

where λ and δ are thermal conductivity and thickness of the membrane, respectively.

2. Logarithmic mean temperature difference LMTD:

In order to solve certain heat exchanger problems, engineers often use a logarithmic mean temperature difference (LMTD), which is used to determine the temperature driving force for heat transfer in heat exchangers. LMTD is introduced due to the fact, the temperature change that takes place across the heat exchanger from the entrance to the exit is not linear.

2.1. Definition of LMTD*:* The term LMTD stands for logarithmic mean temperature difference, which is the logarithmic mean of the difference between the inlet and outlet temperatures for hot and cold fluids inside the heat exchanger.

The log mean temperature difference formula is:

$$\Delta T_{LM} = \frac{(\Delta T_1 - \Delta T_2)}{ln\left(\frac{\Delta T_1}{\Delta T_2}\right)} \quad \text{(I.23)}$$

Where:

- ΔT_1 and ΔT_2 Temperature differences for fluids at the inlet and outlet of the heat exchanger.
- ΔT_{lm} Logarithmic mean temperature difference.

2.2. The formula for LMTD – counter-flow and parallel-flow:

The variation in the LMTD formula for these two types of flow depends on the inlet and outlets. The formula for the temperature difference terms ΔT_1 and ΔT_2 vary as per the flow. However, the convention is temperature difference at left and right sides, respectively.

➢ ***LMTD for Parallel-flow:*** Since the flow direction of both fluids is the same, the formula is:

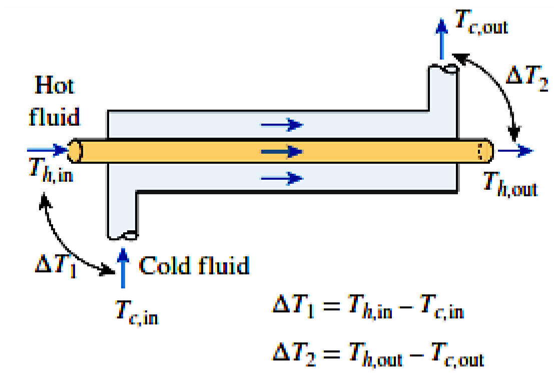

Figure I.10 the expressions ΔT_1 and ΔT_2 in parallel-flow heat exchangers.

Where*:*

- T_{hi} Temperature of the hot fluid at the inlet.
- T_{ho} Temperature of the hot fluid at the outlet.
- T_{ci} Temperature of the cold fluid at the inlet.
- T_{co} Temperature of the cold fluid at the outlet.

Development of LMTD for Parallel-flow:

$$\partial Q = -\dot{m}_h C_{ph} dT_h \quad \text{(I.24)}$$

$$\partial Q = -\dot{m}_c C_{pc} dT_c \quad \text{(I.25)}$$

$$\partial Q = -\dot{m}_h C_{ph} dT_h \Rightarrow dT_h = -\frac{\partial Q}{\dot{m}_h C_{ph}} \quad \text{(I.26)}$$

$$\partial Q = -\dot{m}_c C_{pc} dT_c \Rightarrow dT_c = -\frac{\partial Q}{\dot{m}_c C_{pc}} \quad \text{(I.27)}$$

$$dT_h - dT_c = d(T_h - T_c) \quad \text{(I.28)}$$

Putting (I.26) and (I.27) into (I.28), we get:

$$-\left(\frac{\partial Q}{\dot{m}_h C_{ph}} + \frac{\partial Q}{\dot{m}_c C_{pc}}\right) = -\partial Q\left(\frac{1}{\dot{m}_h C_{ph}} + \frac{1}{\dot{m}_c C_{pc}}\right) \quad \text{(I.29)}$$

$$\partial Q = U(T_h - T_c)\partial A_s \quad \text{(I.30)}$$

$$d(T_h - T_c) = -U(T_h - T_c)\partial A_s\left(\frac{1}{\dot{m}_h C_{ph}} + \frac{1}{\dot{m}_c C_{pc}}\right) \quad \text{(I.31)}$$

$$\frac{d(T_h - T_c)}{(T_h - T_c)} = -U dA_s\left(\frac{1}{\dot{m}_h C_{ph}} + \frac{1}{\dot{m}_c C_{pc}}\right) \quad \text{(I.32)}$$

$$ln\frac{(T_{h,out} - T_{c,out})}{(T_{h,in} - T_{c,in})} = -U dA_s\left(\frac{1}{\dot{m}_h C_{ph}} + \frac{1}{\dot{m}_c C_{pc}}\right) \quad \text{(I.33)}$$

$$Q = -\dot{m}_h C_{ph}(T_{h,in} - T_{h,out}) \Rightarrow \frac{1}{\dot{m}_h C_{ph}} = \frac{T_{h,in} - T_{h,out}}{Q} \quad \text{(I.34)}$$

$$Q = -\dot{m}_c C_{pc}(T_{c,out} - T_{c,in}) \Rightarrow \frac{1}{\dot{m}_c C_{pc}} = \frac{T_{c,out} - T_{c,in}}{Q} \quad \text{(I.35)}$$

$$ln\frac{(T_{h,out} - T_{c,out})}{(T_{h,in} - T_{c,in})} = -UA_s\left(\frac{T_{h,in} - T_{h,out}}{Q} + \frac{T_{C,out} - T_{c,in}}{Q}\right) \quad \text{(I.36)}$$

$$ln\frac{(T_{h,out} - T_{c,out})}{(T_{h,in} - T_{c,in})} = -\frac{UA_s}{Q}\left((T_{h,in} - T_{h,out}) + (T_{c,out} - T_{c,in})\right) \quad \text{(I.37)}$$

$$ln\frac{(T_{h,out} - T_{c,out})}{(T_{h,in} - T_{c,in})} = \frac{UA_s}{Q}(T_{h,out} - T_{c,out} - T_{h,in} - T_{c,in}) \quad \text{(I.38)}$$

$$\Delta T_1 = (T_{h,in} - T_{c,in}) \quad \& \quad \Delta T_2 = (T_{h,out} - T_{c,out}) \quad \text{(I.39)}$$

$$Q = UA_s \Delta T_{LM} \ \ avec \ \ \Delta T_{LM} = \frac{(\Delta T_1 - \Delta T_2)}{ln\left(\frac{\Delta T_1}{\Delta T_2}\right)} \quad \text{(I.40)}$$

- ***LMTD for counter-flow:*** Here, the flow direction of both fluids is different. In this case, the inlet of hot fluid and outlet of cold fluid is on the same side (left) of the heat exchanger. Therefore, the formula is:

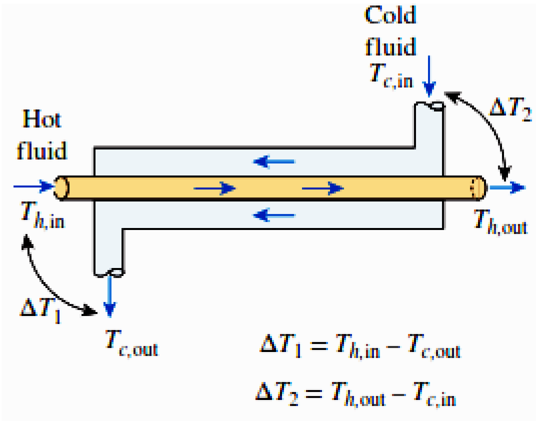

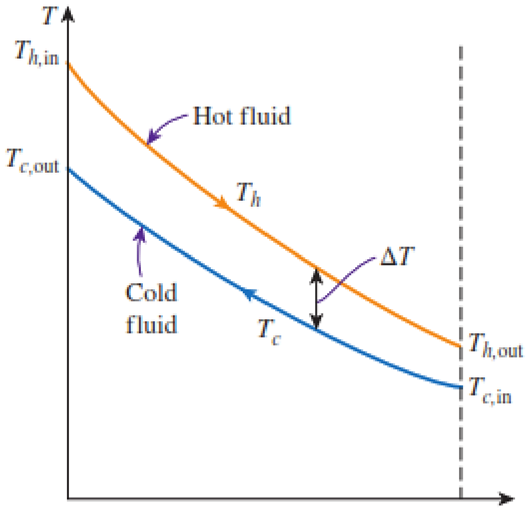

Figure I.11: the expressions ΔT_1 and ΔT_2 in and the variation of fluid temperatures in a counter-flow heat exchanger.

Development of LMTD for counter-flow:

$$\partial Q = U\partial A(T_h - T_c) \quad \textbf{(I.41)}$$

$$\partial Q = -\dot{m}_h C_{ph} dT_h \;\Rightarrow dT_h = -\frac{\partial Q}{\dot{m}_h C_{ph}} \quad \textbf{(I.42)}$$

$$\partial Q = -\dot{m}_c C_{pc} dT_c \Rightarrow dT_c = -\frac{\partial Q}{\dot{m}_c C_{pc}} \quad \textbf{(I.43)}$$

$$dT_h - dT_c = d(T_h - T_c) = -\frac{\partial Q}{\dot{m}_h C_{ph}} + \frac{\partial Q}{\dot{m}_c C_{pc}} \quad \textbf{(I.44)}$$

$$d(T_h - T_c) = -\partial Q\left(\frac{1}{\dot{m}_h C_{ph}} - \frac{1}{\dot{m}_c C_{pc}}\right) \quad \textbf{(I.45)}$$

$$d(T_h - T_c) = -U\partial A(T_h - T_c)\left(\frac{1}{\dot{m}_h C_{ph}} - \frac{1}{\dot{m}_c C_{pc}}\right) \quad \textbf{(I.46)}$$

$$\int_i^o \frac{d(T_h - T_c)}{T_h - T_c} = -U\left(\frac{1}{\dot{m}_h C_{ph}} - \frac{1}{\dot{m}_c C_{pc}}\right)\int_i^o \partial A \quad \textbf{(I.47)}$$

$$[\ln(T_h - T_c)]_i^o = -UA\left(\frac{1}{\dot{m}_h C_{ph}} - \frac{1}{\dot{m}_c C_{pc}}\right) \quad \textbf{(I.48)}$$

$$\ln\left(\frac{T_{ho} - T_{ci}}{T_{hi} - T_{co}}\right) = -UA\left(\left(\frac{T_{hi} - T_{ho}}{Q}\right) - \left(\frac{T_{co} - T_{ci}}{Q}\right)\right) \quad \textbf{(I.49)}$$

$$\ln\left(\frac{T_{ho} - T_{ci}}{T_{hi} - T_{co}}\right) = -\frac{UA}{Q}\left(-(T_{hi} - T_{ho}) + (T_{co} - T_{ci})\right) \quad \textbf{(I.50)}$$

$$\boldsymbol{ln\left(\frac{T_{ho}-T_{ci}}{T_{hi}-T_{co}}\right)=\frac{UA}{Q}(-T_{hi}+T_{ho}+T_{co}-T_{ci})} \qquad \textbf{(I.51)}$$

$$\boldsymbol{ln\left(\frac{T_{ho}-T_{ci}}{T_{hi}-T_{co}}\right)=\frac{UA}{Q}\left((T_{ho}-T_{ci})-(T_{hi}-T_{co})\right)} \qquad \textbf{(I.52)}$$

$$\boldsymbol{\Delta T_1=T_{hi}-T_{co}\& \qquad \Delta T_2=T_{ho}-T_{ci}} \qquad \textbf{(I.53)}$$

$$\boldsymbol{ln\frac{\Delta T_2}{\Delta T_1}=\frac{UA}{Q}(\Delta T_2-\Delta T_1)} \qquad \textbf{(I.54)}$$

$$\boldsymbol{Q=UA_s\Delta T_{LM}} \quad \text{with} \quad \boldsymbol{\Delta T_{LM}=\frac{(\Delta T_2-\Delta T_1)}{ln\left(\frac{\Delta T_2}{\Delta T_1}\right)}} \qquad \textbf{(I.55)}$$

- **Counter-flow vs parallel-flow:** Assuming the same set of inlet and outlet temperatures, the LMTD value for counter-flow would be greater than the parallel one. Therefore, it would have lesser surface area for the same amount of heat transfer.

- **LMTD for multipass and cross-flow*:*** In addition to the parallel and counter-flow heat exchangers, there are much more complex versions where the fluids pass multiple times, i.e., multipass or flowing perpendicular to each other, i.e., cross-flow. The shell and tube heat exchanger diagram can be seen below, along with different types of heat exchangers.

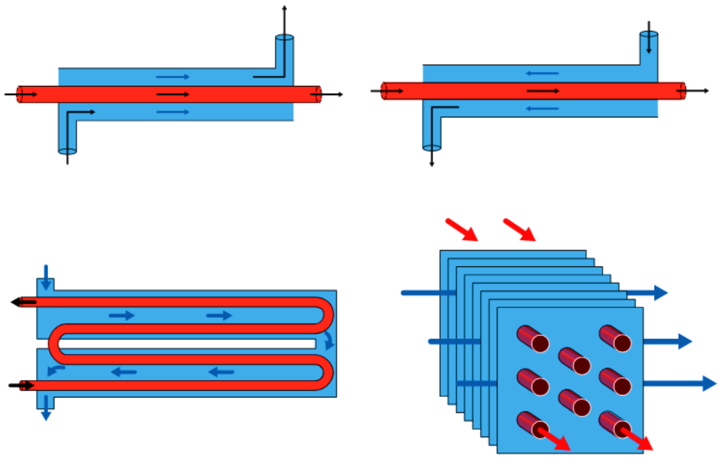

Figure I.12: *Types of heat exchangers — (clockwise from top left) parallel-flow, counter-flow, cross-flow, and shell and tube heat exchangers.*

To calculate LMTD for the said configurations, a term called correction factor, F, is introduced in the equation below: $\Delta T_{LM} = \Delta T_{LM,cf}$

where:

ΔT_{LMTD} – LMTD value for the cross-flow or shell and tube heat exchangers**.**

- $\Delta T_{lm,cf}$ – LMTD value for counter-flow arrangement.

Therefore, the steps in the case of these advanced heat exchangers are:

- Calculate the LMTD considering the counter-flow arrangement.
- Apply the correction factor.

$$\Delta T_1 = T_{h,in} - T_{c,out}$$
$$\Delta T_2 = T_{h,out} - T_{c,in}$$

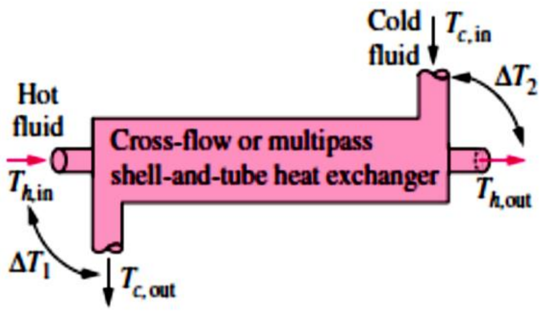

Figure I.13: the expressions ΔT_1 and ΔT_2 in multipass and cross-flow in heat exchanger.

$$\begin{cases}\Delta T_1 = T_{h,in} - T_{c,out} \\ \Delta T_2 = T_{h,out} - T_{c,in}\end{cases} \Rightarrow \Delta T_{LM,cf} = \frac{(\Delta T_2 - \Delta T_1)}{ln\left(\frac{\Delta T_2}{\Delta T_1}\right)} \Rightarrow Q = F\ U\ A_s \Delta T_{LM,cf} \quad \textbf{(I.56)}$$

F: is the correction factor, which depends on the geometry of the heat exchanger and the inlet and outlet temperatures of the hot and cold fluid flows.

$$F = \frac{\frac{\sqrt{R^2+1}}{R-1} ln\left(\frac{1-P}{1-P.R}\right)}{ln\left(\frac{\left(\frac{2}{P}\right)-1-R+\sqrt{R^2+1}}{\left(\frac{2}{P}\right)-1-R-\sqrt{R^2+1}}\right)} \quad \textbf{(I.57)}$$

You can obtain correction factor from the charts based on two parameters, P and R. Such that:

$$P = \frac{t_2 - t_1}{T_1 - t_1} \quad \textbf{(I.58)}$$

$$R = \frac{T_1 - T_2}{t_2 - t_1} = \frac{(\dot{m}C_p)_{tube\ side}}{(\dot{m}C_p)_{calander\ side}} \quad \textbf{(I.59)}$$

where:

- t_1 and t_2 – Inlet and outlet temperature for shell side of the heat exchanger.
- T_1 and T_2 – Inlet and outlet temperature for tube side of the heat exchanger.

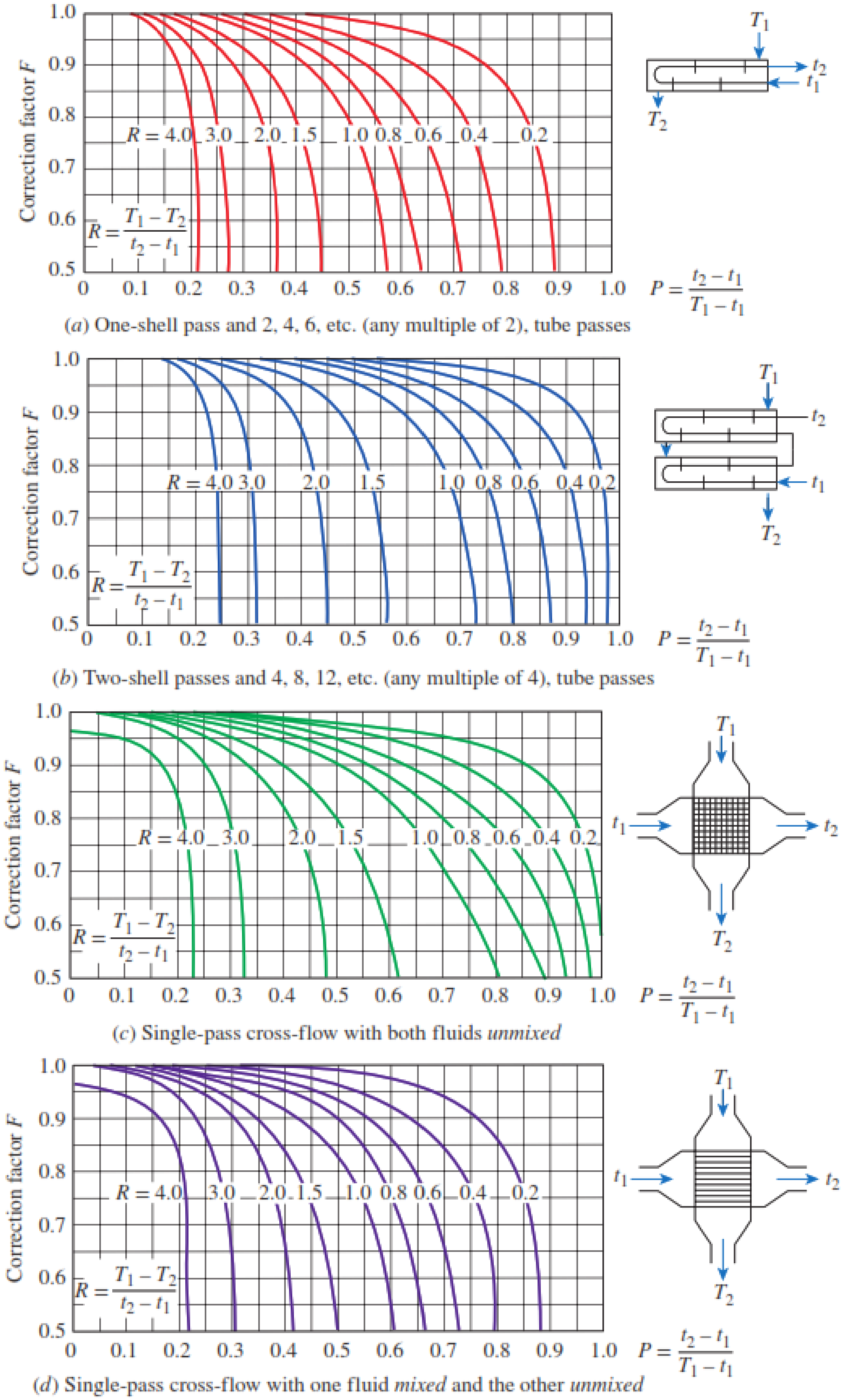

Figure I.14: Correction factor F charts for common shell-and-tube and crossflow heat exchangers. Source: Bowman, Mueller, and Nagle, 1940.

The values of P and R are used along with the configuration of the heat exchangers, e.g., fluid through shell passes once, but 2 times for the fluid in the tube. Then, you should refer to the chart for the above arrangement and use the P and R values to obtain the correction factor. Some of the charts can be seen below.

2.3 Effective–NTU (ε-NTU) method:

When the heat transfer rate is not known or the outlet temperatures are not known tedious iterations with the LMTD method are required. In an attempt to eliminate the iterations, Kays and London in 1955 developed a new method called the effective-NTU method. Current practice tends to favor the effectiveness approach because both effectiveness and the number of transfer units have a unique physical significance for a given exchanger and given flow thermal capacities.

2.3.1 Heat transfer rate:

The E-NTU model defines the heat transfer rate between fluids cold and hot in terms of an effectiveness parameter ε:

$$\boldsymbol{Q1} = \boldsymbol{Q2} = \boldsymbol{\varepsilon Qmax}\,, \quad \mathbf{0} < \varepsilon < 1$$

where:

- Q_1 and Q_2 are the heat transfer rates into cold fluid and hot fluid.
- Q_{max} is the maximum possible heat transfer rate between cold fluid and hot fluid at a given set of operating conditions.
- ε is the effectiveness parameter.

The maximum possible heat transfer rate between the two fluids is:

$$\boldsymbol{Qmax} = \boldsymbol{Cmin}\Delta\mathbf{T_{max}} \qquad \textbf{(I.60)}$$

$$\Delta\mathbf{T_{max}} = (\boldsymbol{T1}_{,}\boldsymbol{In} - \boldsymbol{T2}_{,}\boldsymbol{In}) \qquad \textbf{(I.61)}$$

where:

- C_{min} is the minimum value of the thermal capacity rate:

$$\boldsymbol{C_{min}} = \mathbf{min}\left(\boldsymbol{\dot{m}_{cold}C_{p,cold}}\,, \boldsymbol{\dot{m}_{hot}C_{p,hot}}\right) \qquad \textbf{(I.62)}$$

the maximum temperature difference $(T_{1,in} - T_{2,in})$

- $T_{1,in}$ and $T_{2,in}$ are the inlet temperatures of fluid 1 and fluid 2.
- $\dot{m}_{cold}$ and $\dot{m}_{hot}$ are the mass flow rates of fluid 1 and fluid 2 into the heat exchanger volume through the inlet.
- $c_{p,1}$ and $c_{p,2}$ are the specific heat coefficients at constant pressure of cold fluid and hot fluid. The minimum fluid-wall heat transfer coefficient parameter in the block dialog box sets a lower bound on the allowed values of the heat transfer coefficients.

The heat exchanger effectiveness ε is then written by:

$$\boldsymbol{\varepsilon = \frac{Actual\ Heat\ Transfer\ Rate}{Maximum\ Possible\ Heat\ Transfer\ Rate} = \frac{Q_{real}}{Q_{max}} = \frac{T_{c,in}-T_{c,out}}{T_{c,in}-T_{h,out}}} \quad \textbf{(I.63)}$$

$$\boldsymbol{Q_{real} = \dot{m}_c C_{P,c}(T_{c,out} - T_{c,in}) = \dot{m}_h C_{P,h}(T_{c,in} - T_{c,out})} \quad \textbf{(I.64)}$$

2.3.2. Heat exchanger effectiveness:

The heat exchanger effectiveness calculations depend on the flow arrangement type selected in the block dialog box. For all but Generic — effectiveness table, the block computes the thermal exchange effectiveness through analytical expressions written in terms of the number of transfer units (NTU) and thermal capacity ratio. The number of transfer units is defined as:

$$\boldsymbol{NTU = \frac{UA}{C_{min}} = \frac{1}{C_{min}R_{Overall}}} \quad \textbf{(I.65)}$$

where:

- NTU is the number of transfer units.
- U is the overall heat transfer coefficient between cold fluid and hot fluid .
- R_{Overall} is the overall thermal resistance between cold fluid and hot fluid.
- A is aggregate area of the primary and secondary, or finned, heat transfer surfaces.

The thermal capacity ratio is defined as

$$\boldsymbol{C_{real} = \frac{C_{min}}{C_{max}}} \quad \textbf{(I.66)}$$

where:

- C_{real} is the thermal capacity ratio.

The overall heat transfer coefficient and thermal resistance used in the NTU calculation are functions of the heat transfer mechanisms at work. These mechanisms include convective heat transfer between the fluids and the heat exchanger interface and conduction through the interface wall

$$\boldsymbol{R_{Overall} = \frac{1}{UA} = \frac{1}{h_{cold}A_{cold}} + R_{foul,cold} + R_{wall} + R_{foul,hot} + \frac{1}{h_{hot}A_{hot}}} \quad \textbf{(I.67)}$$

where:

- h_1 and h_2 are the heat transfer coefficients between fluid 1 and the interface wall and between fluid 2 and the interface wall.
- $A_{,\text{cold}}$ and A_{hot} are the heat transfer surface areas on the fluid-cold and fluid-hot sides.
- $R_{\text{foul,cold}}$ and $R_{\text{foul,hot}}$ are the fouling resistances on the fluid-cold and fluid-hot sides.
- R_{wall} is the interface wall thermal resistance.

2.3.2.1 Parallel-flow:

Knowing that for a parallel-flow heat exchanger can be rearranged as follows:

$$\boldsymbol{ln}\frac{T_{h,out}-T_{c,out}}{T_{h,in}-T_{c,in}} = -\frac{UA_s}{c_c}\left(1+\frac{C_c}{C_h}\right) \quad \text{(I.68)}$$

And

$$T_{h,out} = T_{h,in} - \frac{C_c}{C_h}\left(T_{c,out}-T_{c,in}\right) \quad \text{(I.69)}$$

Putting (I.68) into (I.69) we get:

$$\boldsymbol{ln}\frac{T_{h,in}-T_{c,in}+T_{c,in}-\frac{C_c}{C_h}(T_{c,out}-T_{c,in})-T_{c,in}}{T_{h,in}-T_{c,in}} = -\frac{UA_s}{C_c}\left(1+\frac{C_c}{C_h}\right) \quad \text{(I.70)}$$

$$\ln\left[1-\left(1+\frac{C_c}{C_h}\right)\frac{T_{c,out}-T_{c,in}}{T_{h,in}-T_{c,in}}\right] = -\frac{UA_s}{C_c}\left(1+\frac{C_c}{C_h}\right) \quad \text{(I.71)}$$

$$\varepsilon = \frac{Q_{real}}{Q_{max}} = \frac{C_c(T_{c,out}-T_{c,in})}{C_{min}(T_{h,in}-T_{c,in})} \Rightarrow \frac{T_{c,out}-T_{c,in}}{T_{h,in}-T_{c,in}} = \varepsilon\frac{C_{min}}{C_c} \quad \text{(I.72)}$$

$$\varepsilon_{\text{parallel-flow}} = \frac{1-exp\left[-\frac{UA_s}{C_c}\left(1+\frac{C_c}{C_h}\right)\right]}{\left(1+\frac{C_c}{C_h}\right)\frac{C_{min}}{C_c}} \quad \text{(I.73)}$$

Solving for NTU for parallel-flow, we have:

$$NTU = -\frac{1}{1+C_{real}}\ln[1-\varepsilon(1+C_r)] \quad \text{(I.74)}$$

Since the same result is obtained for $\dot{m}_{hot}C_{p,hot} < \dot{m}_{cold}C_{p,cold}$ or equivalently:

$$C_{min} = C_{hot} = \dot{m}_{hot}C_{p,hot}$$

Equation (I.26) applies for any case of parallel-flow heat exchanger

2.3.2.2 Counter-flow:

Based on a completely analogous analysis, the heat exchanger effectiveness for counter-flow is obtained as:

$$\varepsilon = \frac{1-exp[-NTU(1-C_r)]}{1+C_{real}exp[-NTU(1-C_r)]} \quad \text{(I.75)}$$

Solving for NTU for counter-flow, we have:

$$NTU = \frac{1}{1-C_r}\ln\left(\frac{1-\varepsilon C_{real}}{1-\varepsilon}\right) \quad \text{(I.76)}$$

Using Equation (I.76) and (I.75), the actual heat transfer rate is expressed in terms of the effectiveness, inlet temperatures and a minimum heat capacity rate.

Type of heat exchanger	Relation of effectiveness
double tube heat exchanger Parallel-Flow	$\varepsilon = \frac{1 - exp[-NUT(1+c)]}{(1+c)}$
double tube heat exchanger counter-Flow	$\varepsilon = \frac{1 - exp[-NUT(1-c)]}{1 - c\, exp[-NUT(1-c)]}$
Single calendar heat exchanger multi passes tube 2, 4,…	$\varepsilon = 2\left\{1 + c + \sqrt{1+c^2}\,\frac{1 + exp\left[-NUT\sqrt{1+c^2}\right]}{1 - c\, exp\left[-NUT\sqrt{1+c^2}\right]}\right\}^{-1}$
Cross-flow heat exchanger single pass whose two fluids are not Brazed	$\varepsilon = 1 - exp\left\{\frac{NUT^{0.22}}{C}[\exp(-cNUT^{0.78}) - 1]\right\}$
Cross-flow heat exchanger single pass whose two fluids C_{max} Brazed and C_{min} not Brazed	$\varepsilon = \frac{1}{c}\{1 - \exp\left(1 - c(1 - exp[-NUT])\right)\}$
Cross-flow heat exchanger single pass whose two fluids C_{min} Brazed and C_{max} not Brazed	$\varepsilon = 1 - \exp\left(-\frac{1}{c}(1 - exp[-cNUT])\right)$
All heat exchanger c=0	$\varepsilon = 1 - \exp(-NUT)$

TABLE I.1: Type of heat exchanger and the relation of effectiveness.

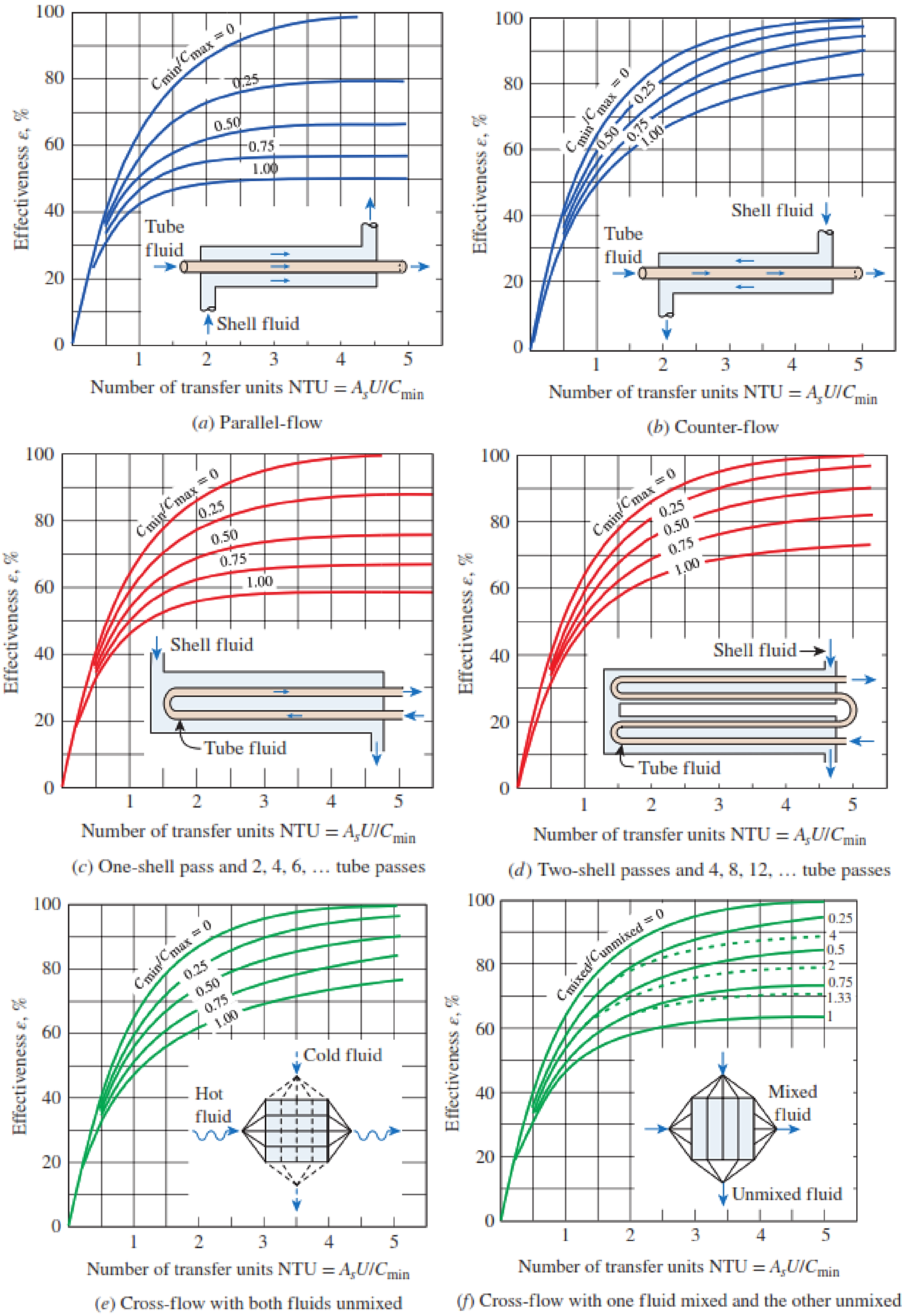

Figure I.15: Effectiveness unit in terms of number of transfers in heat exchangers.

3. Transient heat transfer:

3.1 Definition: It is also known as the Unsteady-state heat transfer Unsteady State Heat Transfer refers to the heat transfer process in which a system's temperature changes with time. This is in contrast to steady-state heat transfer, in which the temperature of a system remains constant over time. Unsteady state heat transfer can occur in various systems, including solid materials, fluids, and gases.

3.2 Theoretical calculation:

$$m_h Cp_h (T_{he} - T_{hs}) dt = U.A_s \Delta T_m dt \quad \textbf{(I.77)}$$

$$\dot{m}_c Cp_c dT_c dt = U.A_s \Delta T_m dt \quad \textbf{(I.78)}$$

As well as the energy balance of the exchanger has the form

$$\dot{m}_h Cp_h (T_{he} - T_{hs}) dt = \dot{m}_c Cp_c dT_c \quad \textbf{(I.79)}$$

Logarithmic Mean Temperature Difference at time t:

$$\Delta T_{LM} = \frac{T_{he} - T_{hs}}{\ln \frac{T_{he} - T_c}{T_{hs} - T_c}} \quad \textbf{(I.80)}$$

putting the equation (I.80) in (I.77), we get:

$$-\frac{U.A_s}{\dot{m}_h Cp_h} = \ln \frac{T_{hs} - T_c}{T_{he} - T_c} \quad \textbf{(I.81)}$$

here we can explain the temperatureT_{hs} (the outlet temperature of the primary agent at time (t): $T_{hs} = T_c + (T_{he} - T_c) exp\left(-\frac{U.A_s}{\dot{m}_h Cp_h}\right)$ **(I.82)**

The combination of equations (I.79) and (I.82) leads to the phrase

$$\dot{m}_h Cp_h (T_{he} - T_{hs}) \left(1 - exp\left(-\frac{U.A_s}{\dot{m}_h Cp_h}\right)\right) dt = \dot{m}_c Cp_c dT_c \quad \textbf{(I.83)}$$

$$\frac{\dot{m}_h Cp_h}{\dot{m}_c Cp_c} \left(1 - exp\left(-\frac{U.A_s}{\dot{m}_h Cp_h}\right)\right) dt = \frac{dT_c}{(T_{he} - T_{hs})} \quad \textbf{(I.84)}$$

By integrating equation (I.84) in the limits $T_c = T_{ci}$ at ($t = 0$) and $T_c = T_{cf}$ to ($t = t_0$) and giving it a form suitable, we get the following expression:

$$-\frac{U.A_s}{\dot{m}_h Cp_h} = \ln\left(1 - \frac{\dot{m}_c Cp_c}{\dot{m}_h Cp_h t_0} \ln \frac{T_{he} - T_{ci}}{T_{he} - T_{cf}}\right) \quad \textbf{(I.85)}$$

CHAPTER II

PROBLEM AT HAND

Introduction:

The aim of this chapter is to investigate numerically the heat transfer performances that occur in a shell and multipass heat exchanger, with an emphasis on thermal and dynamic evolutions. We accomplished this by examining the temperature distribution and fluid flow patterns in the device, as well as evaluating the heat exchanger's effectiveness by calculating the heat transfer rate between the two fluids and the amount of energy required to operate the device. The effectiveness of the heat exchanger was estimated by comparing the actual heat transfer rate to the maximum possible heat transfer rate, which is calculated as the product of the mass flow rate and the specific heat capacity variations between the two fluids. employing computational fluid dynamics (CFD) software, specifically Ansys.

These findings can be used to optimize the design and operation of the shell and multipass heat exchanger for enhanced heat transfer performances.

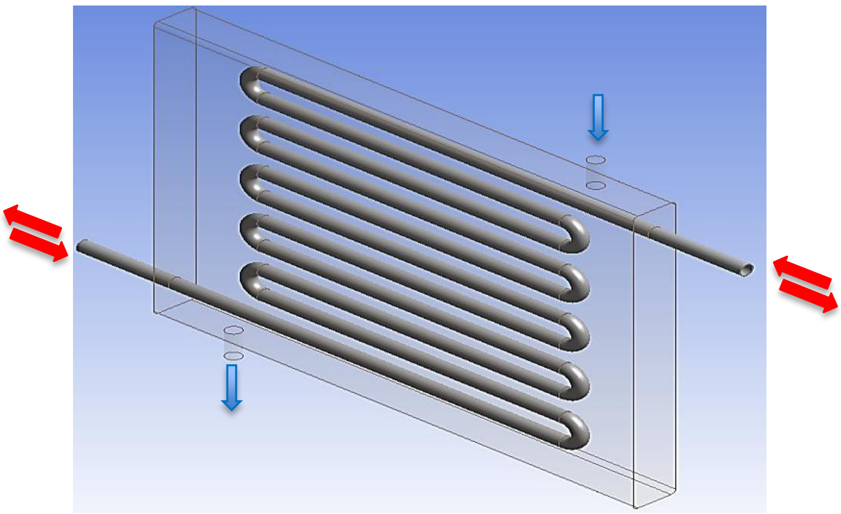

Figure II.1. Our shell multipass tube heat exchanger.

The main objectives of this study can be summarized in two main parts:

- Find the best configuration for maximum heat exchange between two fluids using CFD simulations.
- Conduct a comparative study to identify factors that impact heat exchange and draw conclusion on the best efficiency of the studied cases.

Furthermore, to provide the necessary details for the readers on the development of our numerical model, the most important steps are presented in the following sections in terms of geometry construction, the different functions used for mesh adaptation, and the setup stage of the calculation.

1. Geometry:

In order to create the geometry adopted in our study, we start by using the software design modeler implemented in the ANSYS workbench. The geometry of the heat exchanger chosen is composed of a spiral-type tube of 11 passages with additional entry and exit sections, which are surrounded by a shell that also has entrance and exit sections. The tubes are constructed of copper and have an external diameter of 44mm and a thickness of 1mm, while the shell is built of steel and has dimensions of $1200 \times 1600 \times 150$ mm^3. We followed various steps during that process, which we'll go over below:

- We changed the measurement unit from meter to millimeter (m→mm).
- We began by drawing lines in the (x, y) coordinate system to create the basic shape via the vertical and horizontal lines.

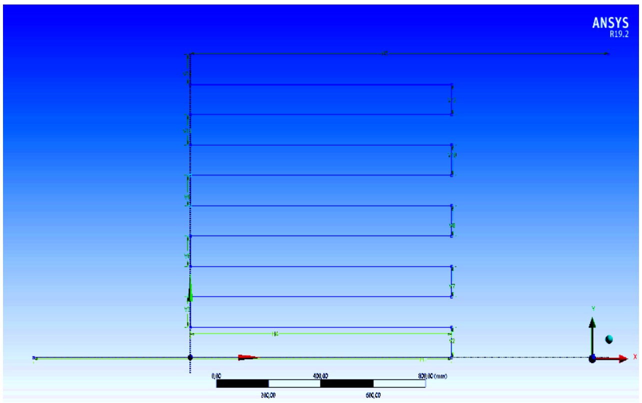

Figure II.1.a. The vertical and horizontal lines.

- Then we have to remove the vertical lines by replacing them with curved ones, using the curved edges tool (acr by 3 points), in order to get the adequate curved serpentine shape of the tube.

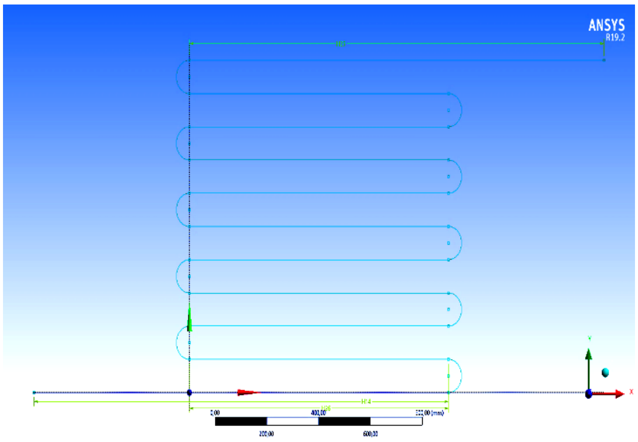

Figure II.1.b. Curved edges (acr by 3 points).

- To assist with drawing position, we included a new (y,z) coordinate system that is shifted by 600mm in the negative X direction, in order to draw two circles one inside another, having diameters of 40mm and 44mm, respectively.

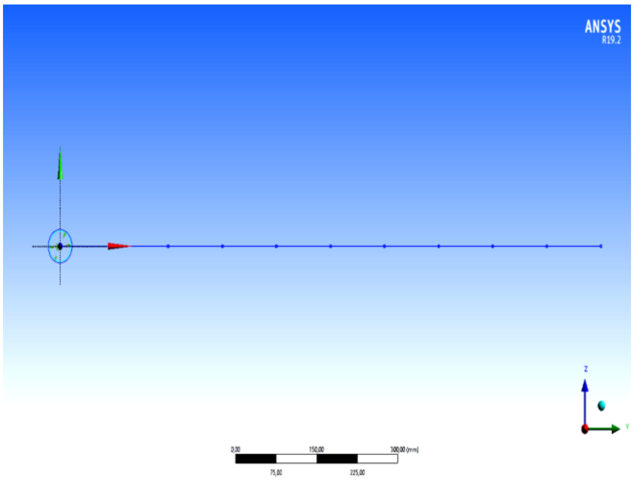

Figure II.1.c. Circle inside another circle.

- The sweeping procedure was carried out by selecting the two circles (the second sketch) as a profile and the first sketch (spiral tubes) as a path that results in the construction of the desired shape.

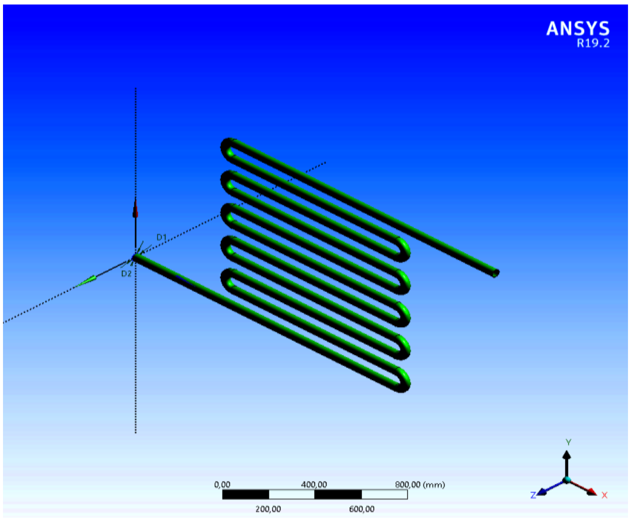

Figure II.1.d. The sweeping procedure.

- Now with the filling tool, we fill the internal content, by selecting all inner surfaces of the tube

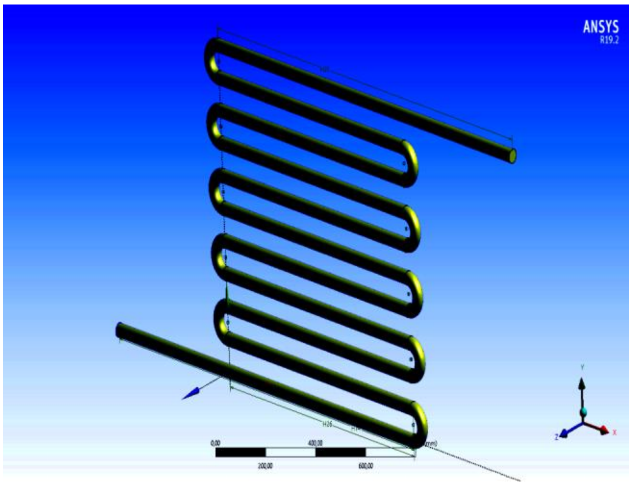

Figure II.1.e. The filling procedure.

After completing the spiral tube drawings, we were meticulous in tracing the processes required to create the right shell for our heat exchanger, which are listed below, stage by stage.

- To begin, we established a new "yz" coordinate system and shifted it roughly -300mm in the x direction before sketching a 1200mm length and 150mm width rectangular to equally encompass the heat exchanger.

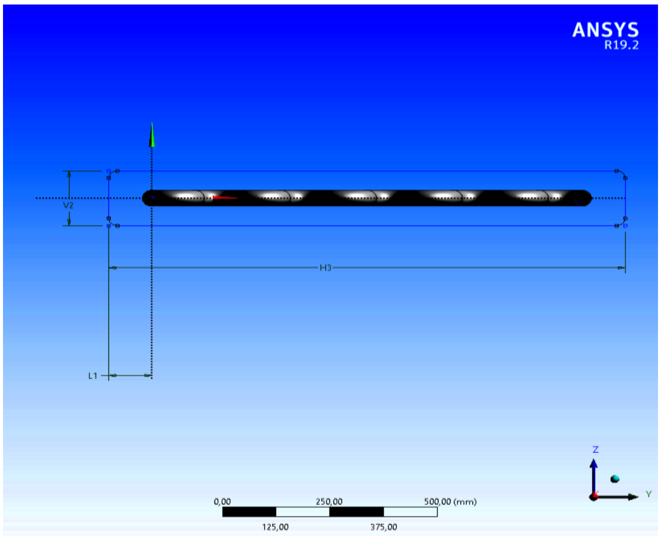

Figure II.1.f. A new "yz" coordinate system.

- We extruded the pre-drawn rectangle and set the depth to 1600mm, and then we generate a full 3D shell with the tubes within and the hot fluid entrance and exit outside the shell.

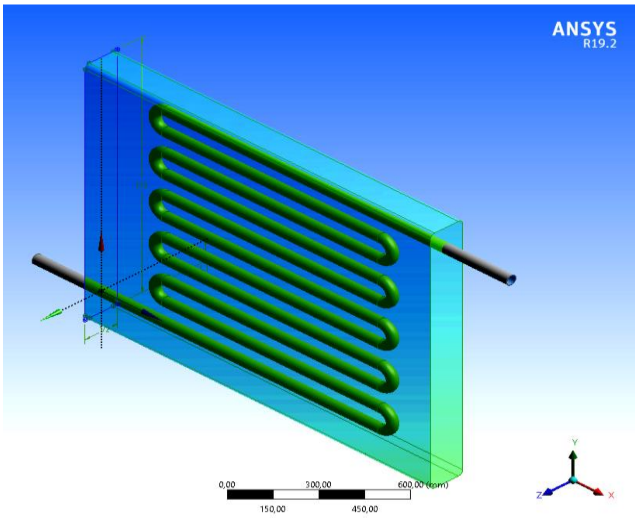

Figure II.1.g. Extrude procedure.

- We drew a coordinate system "zx" and pulled it by 1100mm in the y direction, then drew a circle with a diameter of 55mm and shifted it by 1100mm length in the x direction from the center of the coordinate system, forming a cylinder of length 100mm and connecting it to the surface of the shell.

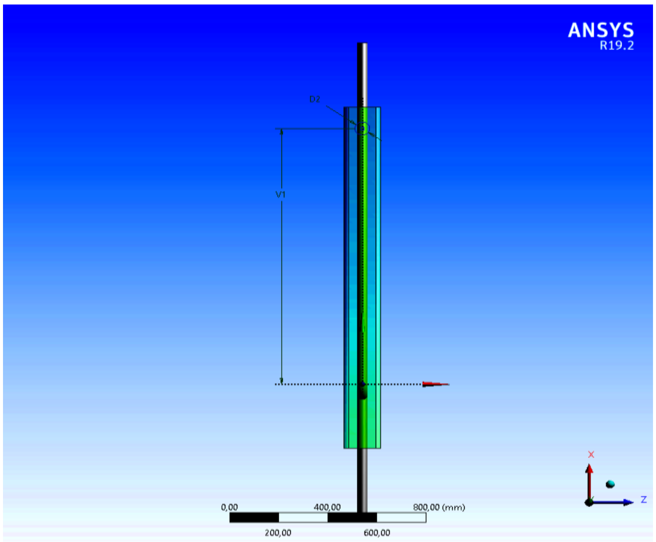

Figure II.1.h. Shell inlet drawing.

- We drew another coordinate system "zx", but this time we pulled it in the y direction by 100mmin the negative direction and drew a circle with a diameter of 55mm on it so that it is 100mm away from the center of the coordinate system in the negative x direction, through extruded the sketch we form a cylinder with a height of 100mm so that it is also connected to the shell.

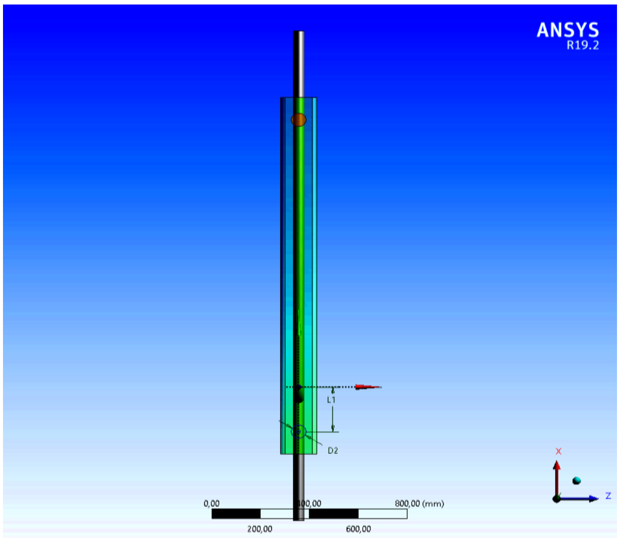

Figure II.1.i. Shell outlet drawing.

- We merged the two cylinders with the shell using the command Boolean, a unit operation, so that they create one shape, and the two cylinders formed the entry and exit of the shell.

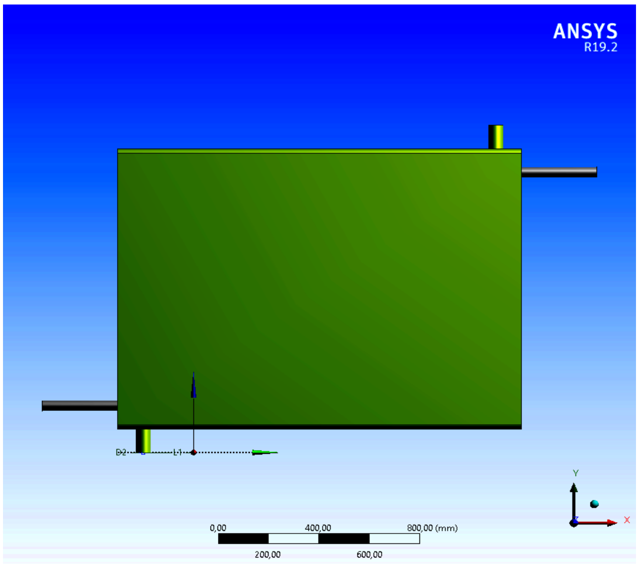

Figure II.1.j. Boolean procedure to merge the two cylinders with the shell.

- We used the shell/surface tool to finish the form. We decided to keep the faces and select all 11 of the shell's outer faces. We added 5mm for thickness and the ability to discard the shape. All of this allowed us to create the final shell shape, which was empty on the inside.

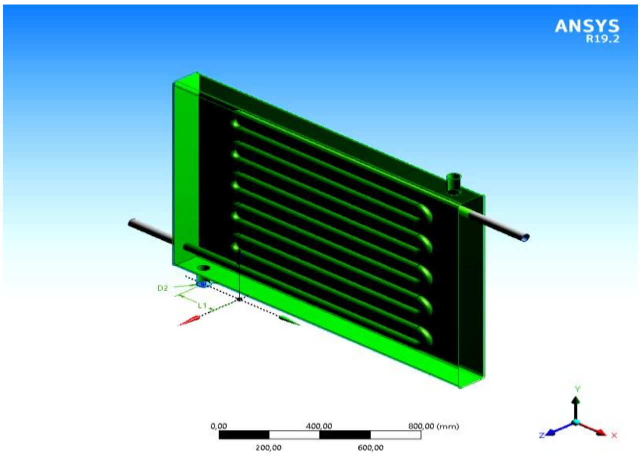

Figure II.1.k. The shell/surface tool.

- Then it was filling time, so we've chosen all of the internal faces of the shell, and it would be filled up how we desired.

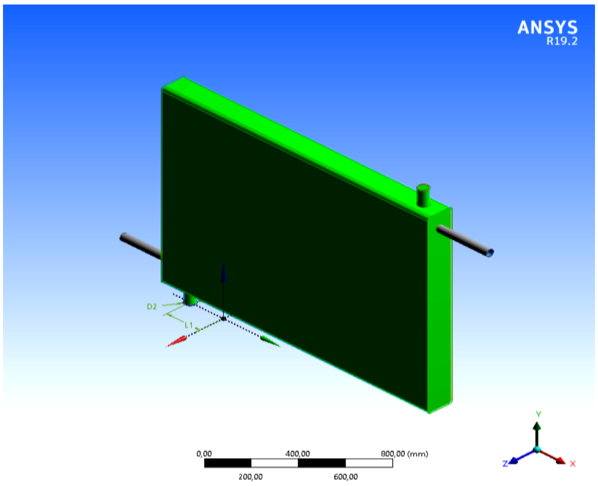

Figure II.1.l. Filling the shape.

- In the final step, we created a Boolean with the subtract option and selected the shape to be separated (the cold liquid) from (shell + tube + hot fluid), with the approval of maintaining the shapes, we got the final shape of the heat exchanger.

Eventually, we received the final heat exchanger, completing the geometry phase with all of its features.

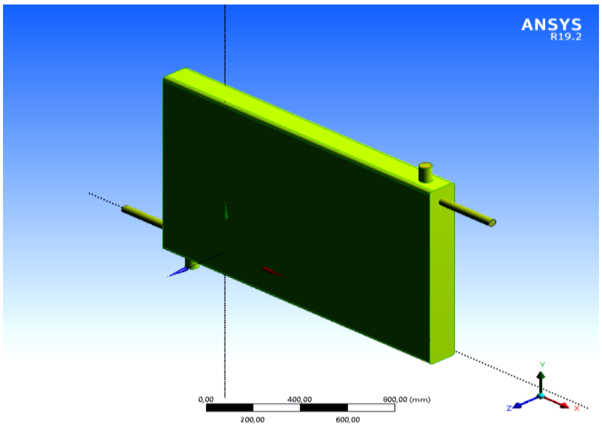

Figure II.1.m. Final shape (shell and multipass tube).

2. Mesh:

Meshing is a crucial step in any computational fluid dynamics (CFD) simulation, including those done using Ansys workbench. In CFD simulations, the geometry of the object being simulated is divided into small elements or cells, which are used to calculate the fluid flow and heat transfer properties. This process is known as meshing. So, the main reason why we mesh the geometry in Ansys workbench is to accurately represent the physical geometry of the object being simulated. An accurate mesh ensures that the CFD simulation results are reliable and provide a realistic representation of the actual physical system.

Meshing also helps to ensure that the computational resources required for the simulation are used efficiently. By dividing the geometry into smaller cells, the simulation can be run on a smaller computational grid, and the simulation time can be reduced.

The type of mesh used in a CFD simulation can also affect the accuracy of the results. For example, a tetrahedral mesh may be more suitable for complex geometries, while a hexahedral mesh may be better for simpler geometries. Therefore, selecting the appropriate mesh method is critical to obtain accurate results.

Therefore, here is a general outline of the process of Meshing a heat exchanger-type shell and multipass tube in Ansys workbench

2.1. Importing the geometry file:

Import the geometry of the heat exchanger into Ansys workbench. This can be done by importing a CAD file or by creating a geometry file within Ansys workbench as we did. Ansys workbench offers several meshing options, including structured, unstructured, and hybrid meshes. For a heat exchanger-type shell and multipass tube, a structured mesh may be preferable, as it can provide better accuracy and control over the mesh size,[8].

- Meshing Quality Metrics: Fluent provides several mesh quality metrics that can be used to evaluate the quality of the mesh. These metrics include aspect ratio, skewness, orthogonality, and smoothness. You can access these metrics in Fluent by using the "Check Mesh" tool.

- Mesh Display Options: Fluent allows you to visualize the mesh using different display options. You can display the mesh using wireframe, surface, or contour plots to help identify any mesh irregularities or distortions.
- Mesh Inspection: Fluent also provides a mesh inspection tool that allows you to inspect the mesh element by element. You can use this tool to identify any inverted, collapsed, or distorted elements in the mesh.

For an accurate calculation, it is more desirable to use a suitable meshing method such as tetrahedral or hexahedral mesh. In our case, we've chosen a hybrid mesh mixed between tetrahedral for the shell and the fluids and hexahedral for the tube to take advantage of their respective strengths. As long as we want our mech to be better, [9].

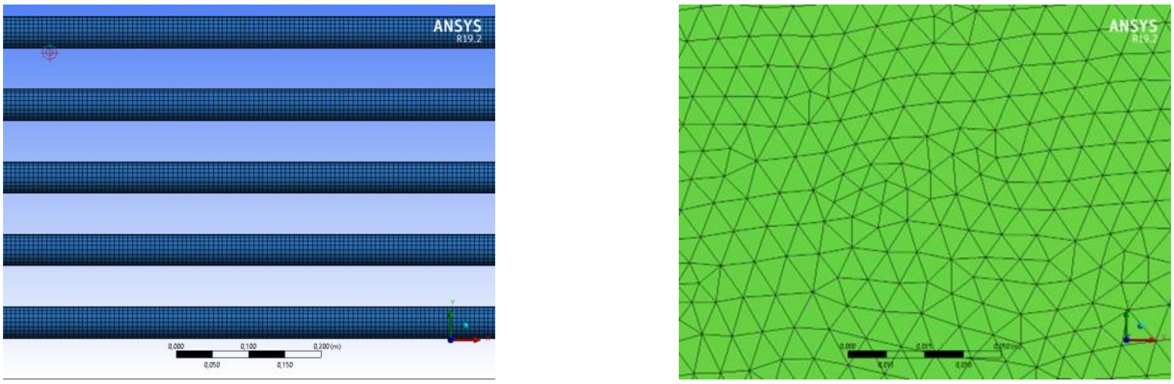

(a) (b)

FigureII.2: (a) hexahedral mesh of the tube part and (b)tetrahedral mesh for the rest of the domain.

2.2. Define the mesh settings:

This step includes specifying the size of the mesh elements and defining the mesh quality controls. So, the element size of 1cm was chosen for our mesh. As a smaller element size provides a higher level of detail but requires more computational resources, while a larger element size reduces computational requirements but can result in lower accuracy and resolution, therefore it's not a good option. That's exactly what happened because the huge size of the heat exchanger that we have, 1200×1600×150 mm^3 dimensions, forced us to avoid utilizing more meshing parameters to refine it, especially since we have a slow computational machine of Intel (R) core™ i7-3770 CPU @ 3.40GHz.

The final mesh statistic gives the number of 3170604 elements, 737115 nodes, with 19 Faces and 6 corps in the mesh, and an overall area of 4.7415 m^2. The minimum element size is 0.1 mm, while the maximum element size is 1cm. It is important to mention that the mesh dependence of the most accurate solution requires further mesh refinement, however, these mesh statistics are relatively more appropriate, given the hyper-large size of the studied domains and our capacity limitation of calculation.

2.3. Define the boundaries of the studied system:

This involves specifying the inlet and outlet boundaries for both the hot and cold fluids and any other boundaries that may be present, such as walls or baffles. Moreover, it is necessary to distinguish the domains of calculation to the surfaces which will be defined as boundary conditions or contact areas. Accordingly, we've defined the inlets and outlets, of both fluids. This is typically done by creating named selections, which allow the boundary conditions to be applied to specific areas of the mesh. In fact, in our case, magnitudes of velocity and specific fixed temperatures are imposed as an inlet boundary condition, and pressure equals zero at those of the outlets. The shell walls were set as adiabatic, meaning that no heat can be transferred through the walls.

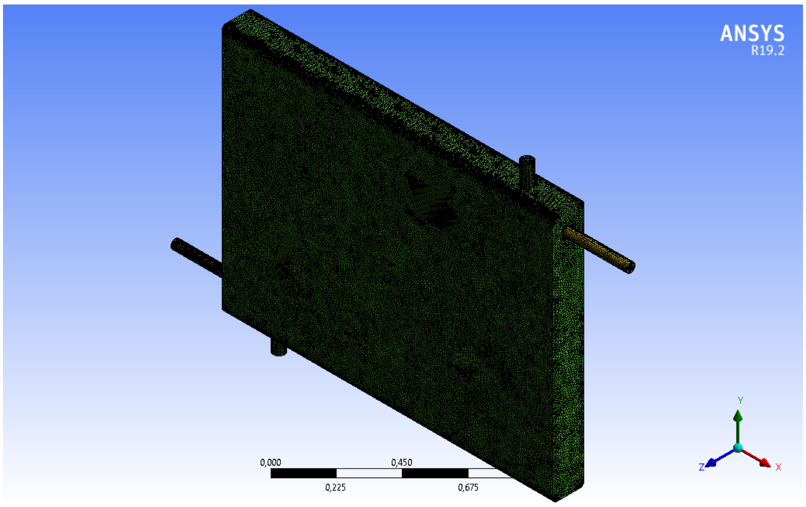

FigureII.3: The final refined mesh.

3. Set up:

3.1. Energy part:

The principle of energy conservation states that energy is neither created nor destroyed. It may transform from one type to another. Like the mass conservation principle, the validity of the conservation of energy relies on experimental observations; thus, it is an empirical law. No experiment has violated the principle of energy conservation yet. The common forms of energy include thermal, mechanical, kinetic, and potential. It may also be stated that the sum of all kinds of energy is constant.

The principle of energy conservation gives the following energy equation

$$\frac{\partial(\rho E)}{\partial t} + \nabla \cdot (\rho E u) = Q - W + \nabla \cdot (\lambda \nabla T) \qquad \textbf{(II.1)}$$

where ρ is the density of the fluid, E is the total energy per unit mass, u is the velocity vector, Q is the rate of heat transfer into the system, W is the work done on the system, λ is the thermal conductivity of the fluid, and T is the temperature.

The total energy per unit mass, E, is given by the following equation:

$$\boldsymbol{E} = \boldsymbol{e} + \frac{\boldsymbol{u}^2}{2} \tag{II.2}$$

Where "e" is the internal energy per unit mass, and $\frac{u^2}{2}$ is the kinetic energy per unit mass.

The first term on the left-hand side of the equation represents the time rate of change of the total energy in the fluid. The second term on the left-hand side represents the advective transport of energy due to the motion of the fluid. The first term on the right-hand side represents the heat transfer rate into the system, while the second term represents the work done on the system. The final term on the right-hand side represents heat diffusion due to thermal conduction, [8].

3.2. Hydrodynamic part:

3.2.1. Continuity equation:

The k-epsilon model assumes that the turbulence is isotropic, meaning that the turbulence properties are the same in all directions. It also assumes that turbulence can be described by two transport equations, one for the turbulent kinetic energy and one for the dissipation rate of turbulent kinetic energy.

The transport equations for k and epsilon are given by

$$\frac{\partial(\rho k)}{\partial t} + \nabla \cdot (\rho k u_i) = P_k - \epsilon + \nabla \cdot (\mu_{eff}\, \nabla k) \tag{II.3}$$

$$\frac{\partial(\rho \epsilon)}{\partial t} + \nabla \cdot (\rho \epsilon u_i) = C_{\epsilon 1} P_k - \frac{C_{\epsilon 2}\rho\epsilon^2}{k} + \nabla \cdot (\mu_{eff} \nabla \epsilon) \tag{II.4}$$

where ρ is the density of the fluid, u_i is the velocity component in the i_{th} direction, P_k is the turbulence production term, ϵ is the dissipation rate of turbulent kinetic energy, μ_{eff} is the effective viscosity, and $C_{\epsilon 1}$ and $C_{\epsilon 1}$ are empirical constants.

The production term, P_k, represents the transfer of energy from the mean flow to the turbulence, while the dissipation term,ϵ, represents the dissipation of turbulent kinetic energy due to the effects of viscosity. The effective viscosity, μ_{eff} is calculated from the turbulent viscosity, μ_t, using a blending function that depends on the distance from solid walls and other factors. [8]

3.2.2. Momentum Equation:

Is a mathematical formula that describes the position, velocity, or acceleration of a body relative to a given frame of reference. Newton's second law, which states that the force F acting on a body is equal to the mass m of the body multiplied by the acceleration an of its Centre of mass, F = ma, is the basic equation of motion in classical mechanics. If the force acting on a body is known as a function of time, also the velocity and position of the body as functions of time can, theoretically, be derived from Newton's equation by a process known as integration. [8]

$$\rho \frac{Du}{Dt} = -\frac{\partial p}{\partial x} + div(\mu grad u) + S_{Mx} \quad \textbf{(II.5-a)}$$

$$\rho \frac{Dv}{Dt} = -\frac{\partial p}{\partial y} + div(\mu grad\, v) + S_{My} \quad \textbf{(II.5-b)}$$

$$\rho \frac{Dw}{Dt} = -\frac{\partial p}{\partial z} + div(\mu grad w) + S_{Mz} \quad \textbf{(II.5-c)}$$

3.2.3 The k-epsilon model:

The k-epsilon model is a turbulence model used in computational fluid dynamics (CFD) to simulate the behavior of turbulent flows. It is one of the most widely used turbulence models due to its simplicity and computational efficiency, and it is suitable for a wide range of turbulent flows, from boundary layers to free shear flows. [8]

The k-epsilon model is based on the idea of separating the turbulent kinetic energy (k) and the rate of dissipation of turbulent kinetic energy (epsilon) from the mean flow variables, and modeling their transport equations separately. The basic equations for the k-epsilon model are:
Transport equation for turbulent kinetic energy k:

$$\frac{\partial \rho k}{\partial t} + \nabla . (\rho k v) = \nabla . [(\mu + \frac{\mu t}{\sigma k}) \nabla k] + P_k - \epsilon \quad \textbf{(II.3)}$$

Transport equation for the rate of dissipation of turbulent kinetic energy epsilon:

$$\frac{\partial \rho \epsilon}{\partial t} + \nabla . (\rho \epsilon v) = \nabla . [(\mu + \frac{\mu t}{\sigma \epsilon}) \nabla \epsilon] + C \epsilon_1 P_k - C \epsilon_1 \frac{\epsilon}{k} \quad \textbf{(II.4)}$$

where:

ρ is. the density of the fluid
v is the velocity vector of the fluid

μ is the dynamic viscosity of the fluid
μ_t is the turbulent viscosity, which is modeled using the turbulent kinetic energy and the rate of dissipation of turbulent kinetic energy
σk and $\sigma \varepsilon$ are the model constants
Pk is the production of turbulent kinetic energy due to mean velocity gradients
ε is the rate of dissipation of turbulent kinetic energy due to viscous effects
$C\varepsilon 1$ and $C\varepsilon 1$ are model constants.
The k-epsilon model is a two-equation model because it solves two transport equations for k and epsilon. These equations are closed by providing additional relations for the turbulent viscosity and the model constants, which are often based on empirical data or assumptions about the nature of the turbulence. [8]

Overall, the k-epsilon model is a popular and effective tool for simulating turbulent flows, and it has been used in a wide range of applications, from aerospace engineering to environmental modeling to biomedical devices. [9]

3.3. Set up of materials used:

Table below, gives the physical properties of all materials used

Materials	Density(kg/m³)	Specific heat(J/kg.°C)	Thermal conductivity (W/m.°C)	Viscosity (Pa.S)
liquid water	998.1	4181	0.6	0.001003
oil	710	3300	0.11	0.01
steel	8030	501.48	16.17	
copper	8978	381	387.6	

Table II.1 Properties of all materials used.

3.4. Set up the cell zone conditions:

We have selected copper and steel for the tubes and the shell, respectively. However, two cases of fluids are numerically examined and will be the subject of comparative study in the next chapter.

- **First case**: Water-Water
- **Second case**: Oil-Water with oil as the hot fluid and Water is the cold one,

3.4.1. Set up the boundary conditions:

we set the temperature to 15°C for each cold fluid in the configurations and 100°C for every hot fluid that will be cooled. Also, we've set the same velocity of 0.1m/s for each fluid in each configuration.

It is important to mention that the fluid configuration of shell and tube is classified as a mixed directions configuration as the present fluids do not have a regular flow direction. Furthermore, in both previously given situations, two fluid configurations are investigated; the first one is a mixed flows with opposing inlets, and the second is a mixed flows with the same inlets. Then we entered 5000 as the number of iterations to ensure that the calculation has achieved convergence and also reached the accuracy wanted.

CHAPTER III

DISCUSSION OF THE RESULTS

Introductions:

The current chapter focuses on the discussion as well as a comparative analysis of the numerical results obtained from the full 3D models which are four different cases of shell and multipass tube heat exchangers. These cases involve the case of water-water and oil-water with both opposite and same inlets. The main objective of this analysis is to evaluate the overall heat transfer characteristics of each type of heat exchanger in terms of temperature field, dynamic field, and finally a thermal efficiency study. By examining these results, the study aims to identify the most suitable heat transfer characteristics for practical applications. The analysis considers various performance metrics, such as the heat transfer coefficient, and overall heat transfer rate. The results are presented and compared through visualizations, including contours, charts, and streamlines. The findings of this study can provide valuable insights into the design and operation of shell and multipass tube heat exchangers, helping engineers to optimize their performance for specific applications.

1. Discussion of the results:

As well-known, heat exchangers usually operate for long periods of time with no change in their operating conditions. Therefore, they can be modeled as steady-flow devices. As such, the mass flow rate of each fluid remains constant, and the fluid properties such as temperature and velocity at any inlet or outlet remain the same. Also, the fluid streams experience little to no change in their velocities and elevations, and thus the kinetic and potential energy changes are negligible. The specific heat of a fluid, in general, changes with temperature. But in a specified temperature range, it can be treated as a constant at some average value with little loss in accuracy. Axial heat conduction along the tube is usually insignificant and can be considered negligible. Finally, the outer surface of the heat exchanger is assumed to be perfectly insulated, so that there is no heat loss to the surrounding medium, and any heat transfer occurs between the two fluids only.

The idealizations stated above are closely approximated in practice, and they greatly simplify the analysis of a heat exchanger with little sacrifice in accuracy. Therefore, they are commonly used. Under these assumptions, the first law of thermodynamics requires that the rate of heat transfer from the hot fluid be equal to the rate of heat transfer to the cold one. That is:

$$Q = m_c Cp_c \left(T_{c,out} - T_{C,in} \right)$$

And

$$Q = m_h Cp_h \left(T_{h,in} - T_{h,out} \right)$$

where the subscripts c and h stand for cold and hot fluids, respectively, and

m_c, m_h = *mass flow rates*

Cp_c, Cp_h = specific heats
$T_{c,out}$, $T_{h,out}$ = outlet temperatures
$T_{c,in}$, $T_{h,in}$ = inlet temperatures

Note that the heat transfer rate Q is taken to be a positive quantity, and its direction is understood to be from the hot fluid to the cold one in accordance with the second law of thermodynamics.

1.1. Temperature Evolution:

After obtaining the numerical results of the four cases of shell and multipass tube heat exchangers, a temperature counter was plotted to examine the temperature evolution of both hot fluid and cold fluid

The results give quantitative and qualitative details on the evolution of the temperature field for all cases. These results will be used in the next section to calculate the efficiency of each heat exchanger configuration in order to identify the most efficient in terms of thermal performance.

1.1.1. Temperature contours analyses:

The temperature analysis of the four cases of shell and tube heat exchangers presented in Figure III.1 shows the temperature variation of both fluids. As expected, for both cases a significant decrease in the temperature of the hot fluid, and against an increase in the cold fluid's temperature, however, this latter never exceeds the outlet temperature of the hot fluid as in the case of the double tube heat exchanger with counterflow configuration. The temperature values of the hot and cold fluids are recorded at various points along the tube and shell, from the inlet to the outlet. The temperature of the hot fluid, which enters the tube with a temperature of 100°C, decreases gradually as it flows through the tube until it reaches the outlet. Similarly, the temperature of the cold fluid, which enters the shell at a temperature of 15°C, increases gradually as it flows through the shell until it reaches the outlet.

In the cases of water-water fluids with the same and opposite inlets, the temperatures of the cold fluid at the shell outlet are 40°C and 41.32°C, respectively. The temperature of the hot fluid outlet at the exit of the pipe is 72.06°C. In the cases of oil-water fluids with opposite and same inlets, the temperature of the cold fluid at the shell outlet is also almost the same, at 36°C and 35.56°C, respectively, while the hot fluid that circulates through the pipe exits it with a temperature of 59.24°C. The results clearly show that in the case of a heat exchanger of shell and multipass tube type, the locations of the inlets and outlets of the two heat transfer fluids, have no real significant effect on the heat exchange, except for a few tenths of a degree. However, it indicates clearly that the case of oil-water characterized by a temperature difference of the hot fluid DT = 40.76 °C, is better compared to the case of water-water, which is DT= 27.94 °C.

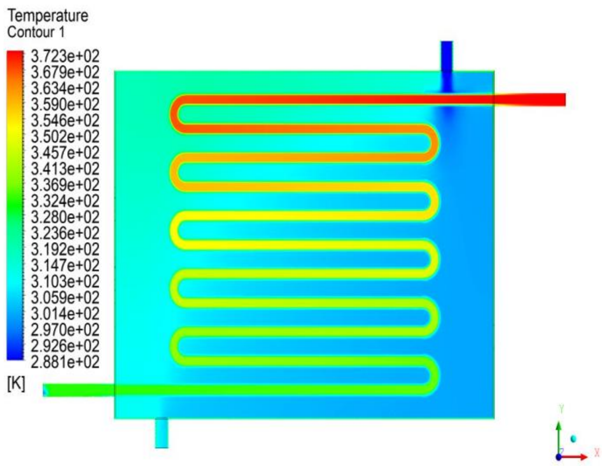

(a) oil-water same input.

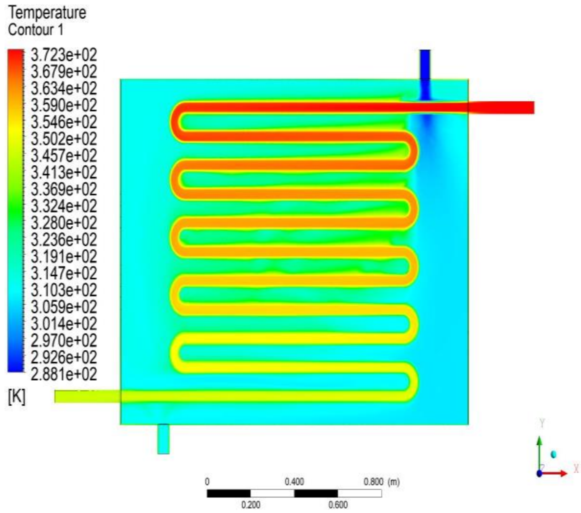

(b) water-water same input.

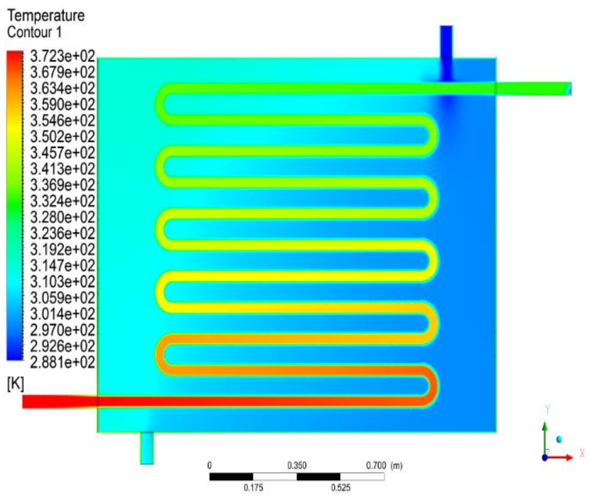

(c) oil-water opposite input.

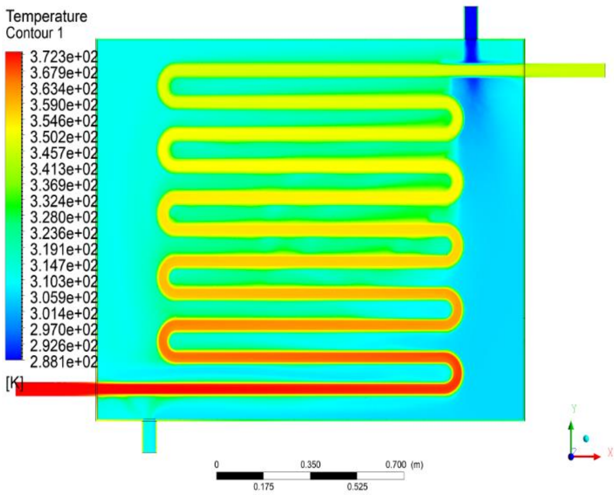

(d) water-water opposite input.

Figure III.1: temperature evolution of heat exchanger between the cold and hot fluid in the four case.

Indeed, in heat exchanger analysis, it is often convenient to combine the product of the mass flow rate and the specific heat of a fluid into a single quantity. This quantity is called the heat capacity rate and is defined for the hot and cold fluid streams as:

For all cases, the specific heat of cold fluid (water), is calculated in a steady regime as follows:

$$C_c = m_c Cp_c = \left(\rho_{water} V_{shell\,inlet} A_{shell\,inlet}\right).Cp_{water} = \left(\rho_{water} V_{Shell\,inlet} \pi \frac{D^2_{shell\,inlet}}{4}\right).Cp_{water}$$

$$= \left(998.1 \times 10^{-1} \times \pi \frac{(0.05)^2}{4}\right) \times 4181 = 819.3776\, W/°C$$

For the case of hot fluid, we have two cases:

- Hot Water

$$C_h = m_h Cp_h = \left(\rho_{water} V_{tube\,inlet} A_{tube\,inlet}\right).Cp_{water} = \left(\rho_{water} V_{tube\,inlet} \pi \frac{D^2_{tube\,inlet}}{4}\right).Cp_{water}$$

$$= \left(998.1 \times 10^{-1} \times \pi \frac{(0.04)^2}{4}\right) \times 4186 = 524.4017\, W/°C$$

- Hot Oil

$$C_h = m_h Cp_h = \left(\rho_{oil} V_{tube\,inlet} A_{tube\,inlet}\right).Cp_{oil} = \left(\rho_{oil} V_{tube\,inlet} \pi \frac{D^2_{tube\,inlet}}{4}\right).Cp_{oil}$$

$$= \left(710 \times 10^{-1} \times \pi \frac{(0.04)^2}{4}\right) \times 3300 = 294.4301\, W/°C$$

The heat capacity rate of a fluid stream represents the rate of heat transfer needed to change the temperature of the fluid stream by 1°C as it flows through a heat exchanger. Note that in a heat exchanger, the fluid with a large heat capacity rate experiences a small temperature change, and the fluid with a small heat capacity rate experiences a large temperature change. Therefore, this approach is consistent with the results obtained indicating that the case of the hot oil will experience the maximum temperature difference.

1.1.2. Charts analyses:

Upon examining the contours of the pictures using the color legend, we observed that the colors gradually decreased, fluctuated, and finally settled at the tube's exit. This fluctuation made it challenging to understand the heat exchange taking place in and around the tube. Hence, we decided to explore other options to gain better insight into the process. We created charts by choosing to follow the evolution of the temperature through a straight line connecting the inlet to the outlet of the shell for the cold fluid, and the evolution of the temperature of the hot fluid through the entire serpentine using the technique of “Point Cloud”, (see the following figure).

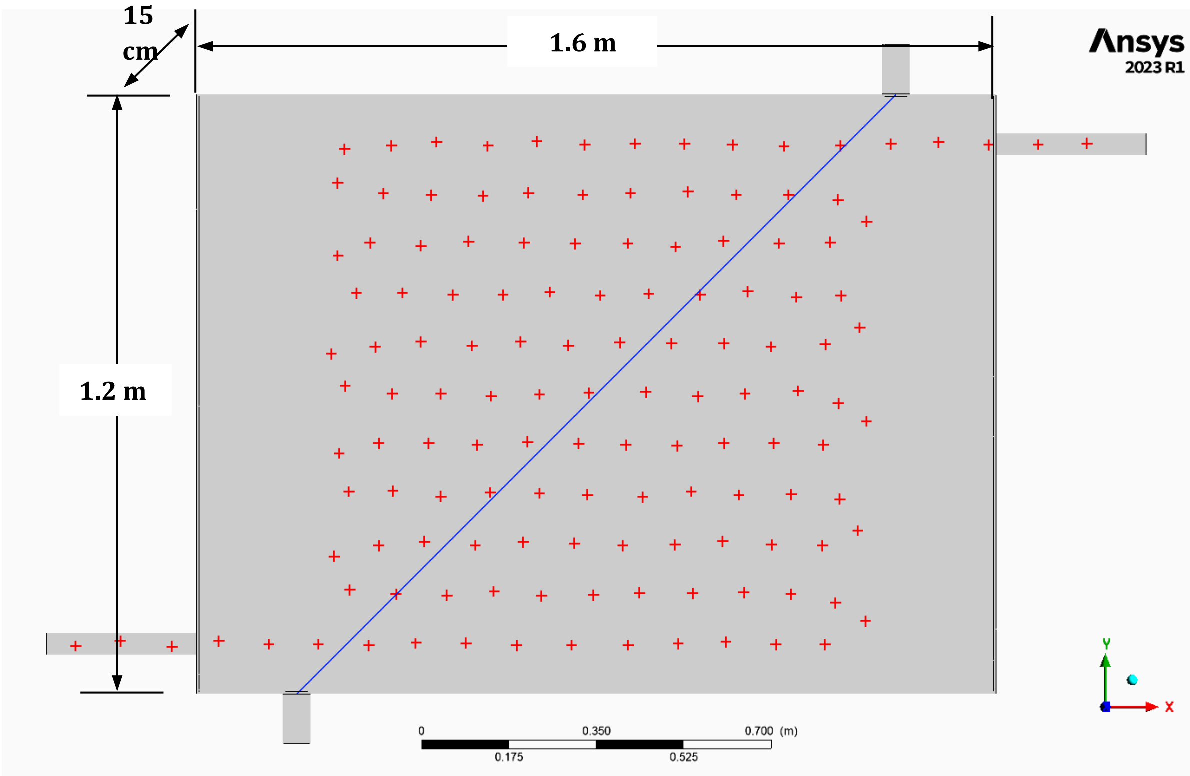

Figure III.2: Technique for monitoring the evolution of temperature for the two heat transfer fluids: blue line from the shell inlet to the outlet for the cold fluid comprising one hundred values and set of pointers of the same number of values for the hot fluid by the Point Cloud technique.

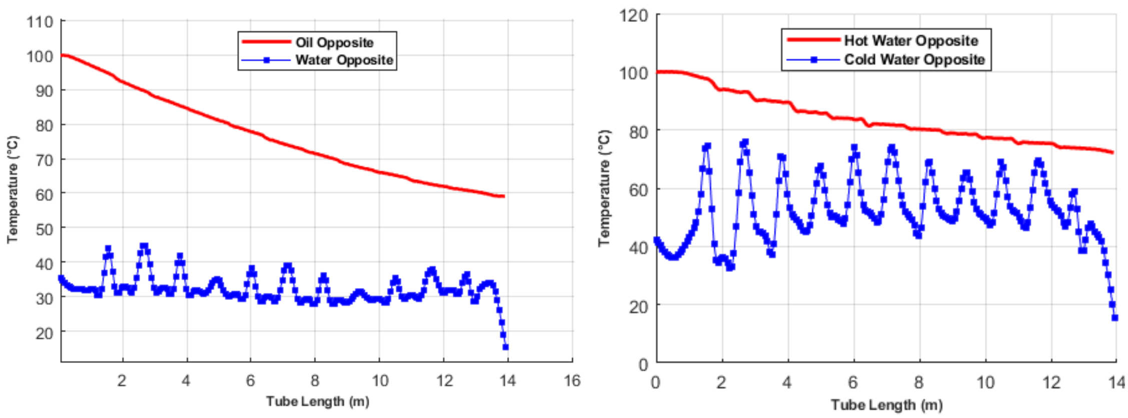

(a) oil-water. *(b)* water-water.

Figure III.3: Temperature evolution of both heat transfer fluids for the case of opposite input: (a) oil-water mixed and (b) water-water.

We see in Figure III.3that the hot fluid (oil) enters at a temperature of 100 °C and progressively decreases until it reaches the exit section at 59.24 °C. While the cold fluid (water) enters at a temperature of 15 °C and fluctuates while it's rising to 35.56 °C on its way out. However, in the case of water-water, the hot fluid (water) enters at 100 °C and then decreases in temperature according to the length of the tube until it reaches the discharge section at 72.06 °C. The cold liquid (water) enters at 15 °C and fluctuates until achieving 42.32 °C as it exits the shell.

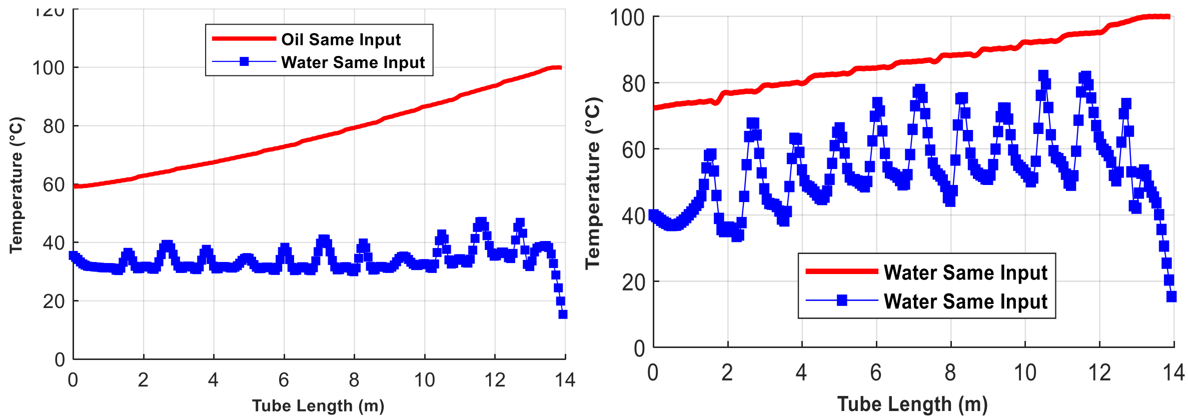

(a) oil-water. (b) water-water.

Figure III.4: Temperature evolution of both heat transfer fluids for the case of the same inputs: (a) oil-water mixed and (b) water-water.

For the case of an oil-water shell multipass tube heat exchanger with the same inputs, Figure III.4 shows that the hot liquid (oil) enters at 100 °C and drops proportionally with tube length until 59.24°C on its way out. The cold liquid (water) enters at 15 °C and fluctuates to reach 35.56 °C on its way to exit. Similarly, in the case of water-water, the hot fluid (water) gets into at a temperature of 100 °C and lowers proportionally to the length of the tube till it reaches the discharge section at 72.06°C. The cold liquid (water) enters at 15 °C and increases in temperature with apparent fluctuations until 42.32 °C as it exits the shell.

In fact, this behavior is in direct relation to the concept of a boundary layer. A simple explanation is that when a fluid flows through a channel or on a surface, a thin layer is formed on the interface between the wall and the fluid. In this thin layer, fluid velocity changes from zero (static) at the wall surface to freestream velocity at a certain distance away from the wall surface. A thick boundary layer has a negative effect on heat exchanger performance as it impedes heat transfer. Think of it like a blanket, the thicker the blanket, the higher the insulation. This is not ideal for a heat exchanger device as the main objective is to conduct heat between the two existing fluids via a tube surface and vice-versa. Turbulent flow is generally preferred in heat exchanger design. The swirling and diffusive characteristics of turbulent flow enhance heat transfer. Mixing induced by a turbulent flow can also disrupt the growth of the boundary layer on heat exchanger's inner surfaces. However, turbulent flow is often associated with higher pressure drop.

In light of the numerical results obtained, namely the temperature contours, it was found the oil-water configuration is more effective in transferring heat than the water-water configuration. This is because the hot fluid in the oil-water configuration loses more energy in the form of heat while the cold fluid absorbs more heat in both directions. As a result, this configuration is more suitable and efficient when there is a need for a larger difference in the outlet temperatures between the fluids.

The heat exchanger's design causes the cold fluid's temperature to fluctuate because it enters from the upper side of the shell and interacts with the tube containing the hot liquid. As the cold fluid approaches and touches the tube, its temperature rises due to heat transfer through the tube wall. The cold fluid then gradually cools down again as it moves away from the tube until it exits the shell. Simply, the hot liquid in the tube acts as the heat source for the cold fluid in the shell side of the heat exchanger, causing the cold fluid's temperature to increase and then decrease.

1.2. Dynamic evolution

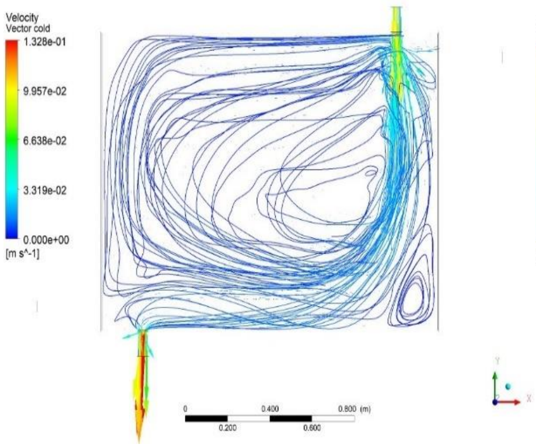

(a) Cold fluid streamlines.

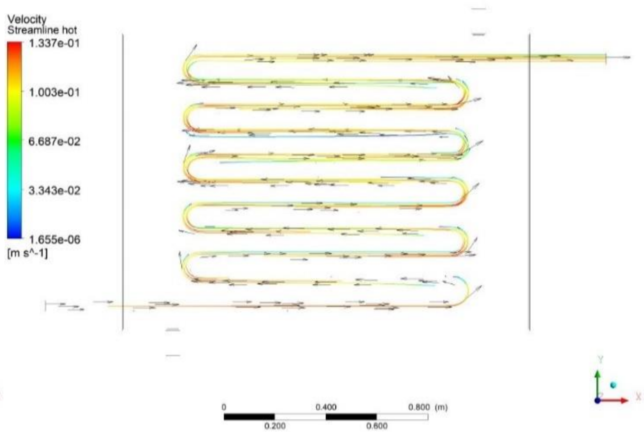

(b) Hot water streamlines.

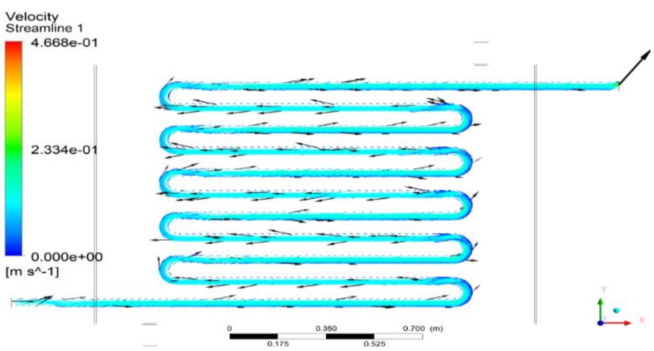

(c) Hot oil streamlines.

Figure III.5: Streamlines of all cases: (a) Cold fluid streamlines, (b)Hot water streamlines, and (c)Hot oil streamlines.

Moreover, as the Reynolds number formula suggests $\left(Re = \frac{\rho V D}{\mu}\right)$, we have in the case of water-water shell and multipass tube heat exchanger, the following calculation:

$$\boldsymbol{v = 0.1\frac{m}{s}\ ; d_o = 0.044m\ ; d_i = 0.040m.}$$

$$\boldsymbol{Re = \frac{\rho \cdot v \cdot d_i}{\mu} \rightarrow Re = \frac{998.1 \times 0.1 \times 0.04}{0.001} = 3992.4;}$$

This value indicates clearly that the flow regime is likely turbulent

And: $\boldsymbol{Pr = \frac{Cp \cdot \mu}{\lambda} \rightarrow \mathrm{Pr} = \frac{4181 \times 0.001}{0.6} = 6.968\ ;}$

$$\boldsymbol{Nu = 0.023 Re^{0.8} \times Pr^{0.3} \rightarrow Nu = 0.023 \times 3992.4^{0.8} \times 6.96^{0.35} = 39.448\ ;}$$

$$\boldsymbol{h_i = \frac{Nu \times \lambda}{d_i} \rightarrow h_i = \frac{39.448 \times 0.6}{0.04} = 591.72\left(\frac{W}{m^2 \cdot {}^\circ C}\right)}$$

flow turbulence is typically achieved at higher fluid velocities. At high Reynolds numbers (in the turbulent regime), there is substantial breaking away of the fluid from the tube and shell walls. This causes significant mixing of the boundary layer and the bulk fluid, enhancing the heat and momentum transfer between the fluid particles.

As mentioned, reducing the size of the boundary layer and promoting turbulent flow can enhance the performance of the heat exchanger. This can be achieved through the following:

- Increase fluid velocity: Speeding up fluid flow through the shell is an effective way of increasing heat transfer. However, the appropriate balance between heat transfer gain and pressure drop penalty needs to be considered. Having closely packed fins and multipass configuration can increase fluid velocity through the core.
- Mixing enhancement features: The addition of features such as turbulators, baffles, and corrugation can further enhance heat transfer.

The same calculation can be used, in order to estimate the flow regime in the case of oil-water shell and multipass tube heat exchanger, as well as the overall heat coefficient of convection inside the tube h_i.

$$\boldsymbol{Re = \frac{\rho \cdot v \cdot d_i}{\mu} \rightarrow Re = \frac{710 \times 0.1 \times 0.04}{0.01} = 284};$$

Against to the case of water, this value indicates clearly that the flow regime is typically laminar

And: $\boldsymbol{Pr = \frac{Cp \cdot \mu}{\lambda} \rightarrow \mathrm{Pr} = \frac{3300 \times 0.01}{0.11} = 300}$;

$$Nu \approx 1.86\left(\frac{\mathrm{Re}.\mathrm{Pr}.L}{D}\right)^{1/3} \rightarrow NU \approx 1.86\left(\frac{284\times300\times13.8}{0.04}\right)^{1/3} = 266.44$$

$$h_i = \frac{Nu \times \lambda}{d_i} \rightarrow h_i = \frac{266.44\times0.11}{0.04} = 732.71\left(\frac{W}{m^2.°C}\right)$$

2. Theoretical calculation:

2.1. Estimation of a correction factor of shell and multipass tube heat exchanger:

In the literature dealing with heat transfer in multipass shell-and-tube heat exchangers, there are a lot of relations developed to estimate the heat flux exchanged and their efficiencies, but the resulting expressions are too complicated because of the complex flow conditions. In such cases, it is convenient to relate the equivalent temperature difference to the log mean temperature difference relation for the counterflow case as:

$$\Delta T_{LM} = F.\Delta T_{LM,CF}$$

where F is the correction factor, which depends on the geometry of the heat exchanger and the inlet and outlet temperatures of the hot and cold fluid streams. The $\Delta T_{lm,\ CF}$ is the log mean temperature difference for the case of a counterflow heat exchanger with the same inlet and outlet temperatures and is determined as flowing

$$\Delta T_{LM,CF} = \frac{\Delta T_1 - \Delta T_2}{\ln\left(\frac{\Delta T_1}{\Delta T_2}\right)}; \quad \begin{cases}\Delta T_1 = T_{h,in} - T_{c,out}\\ \Delta T_2 = T_{h,out} - T_{c,in}\end{cases}$$

The correction factor is less than unity for a multipass shell-and-tube heat exchanger. That is $F \leq 1$. The limiting value of $F = 1$ corresponds to the counterflow heat exchanger. Thus, the correction factor F for a heat exchanger is a measure of the deviation of the ΔT_{lm} from the corresponding values for the counterflow case.

The correction factor F for common shell-and-tube heat exchanger configurations is given in Figure III.6versus two temperature ratios P and R defined as:

$$P = \frac{t_2 - t_1}{T_1 - t_1}$$

$$R = \frac{T_1 - T_2}{t_2 - t_1} = \frac{(m.Cp)_{tube\ side}}{(m.Cp)_{shell\ side}}$$

where the subscripts 1 and 2 represent the inlet and outlet, respectively. Note that for a shell and multipass tube heat exchanger, T and t represent the shell- and tube-side temperatures, respectively, as shown in the correction factor charts.

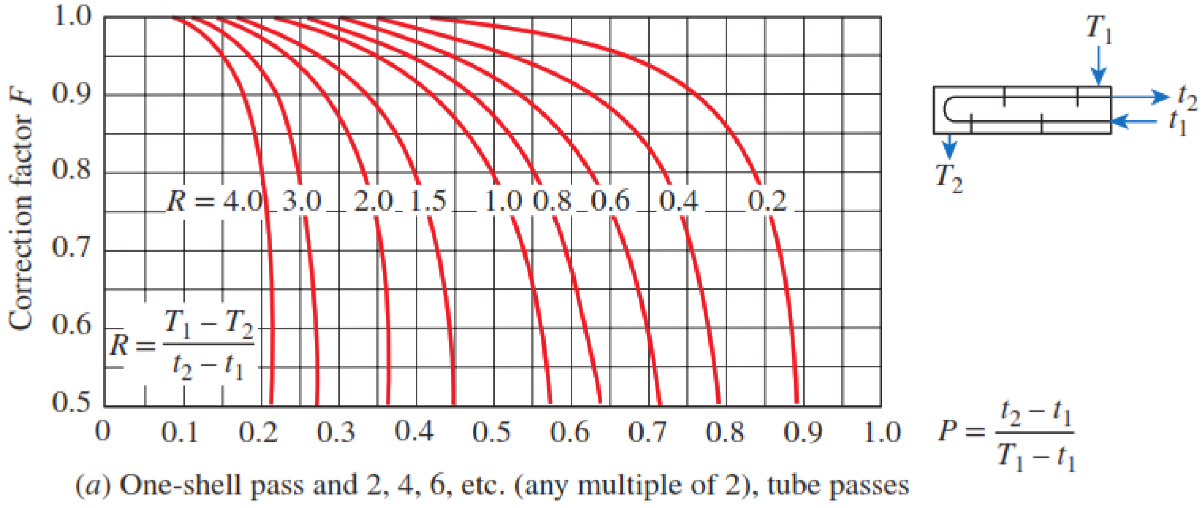

Figure III.6: Correction factor *F* charts for common shell-and-tube heat exchangers.
Source: Bowman, Mueller, and Nagle, 1940.

As a demonstrative example, if we take the case of an oil-water shell and tube heat exchanger with opposite inputs, we have:

$$\mathbf{P = \frac{t_2 - t_1}{T_1 - t_1} = \frac{59.24 - 100}{15 - 100} = 0.4795}$$

$$\mathbf{R = \frac{T_1 - T_2}{t_2 - t_1} = \frac{15 - 35.56}{59.24 - 100} = 0.5044}$$

And we applied the formula of correction factor as:

$$\mathbf{F = \frac{\frac{\sqrt{R^2+1}}{R-1} Ln\left(\frac{1-P}{1-P.R}\right)}{Ln\left(\frac{(2/P)-1-R+\sqrt{R^2+1}}{(2/P)-1-R-\sqrt{R^2+1}}\right)}}$$

$$\mathbf{= \frac{\frac{\sqrt{0.5044^2+1}}{0.5044-1} Ln\left(\frac{1-0.4795}{1-0.4795\times 0.5044}\right)}{Ln\left(\frac{(2/0.4795)-1-0.5044+\sqrt{0.5044^2+1}}{(2/0.4795)-1-0.5044-\sqrt{0.5044^2+1}}\right)} = 0.9492}$$

Similarly, if we take the case of a water-water shell and tube heat exchanger with opposite inputs, we have:

$$P = \frac{t_2 - t_1}{T_1 - t_1} = \frac{72.09 - 100}{15 - 100} = 0.3283$$

$$R = \frac{T_1 - T_2}{t_2 - t_1} = \frac{15 - 42.32}{72.09 - 100} = 0.9788$$

And we applied the formula of correction factor as:

$$F = \frac{\frac{\sqrt{R^2+1}}{R-1} ln\left(\frac{1-P}{1-P\cdot R}\right)}{ln\left(\frac{(2/P)-1-R+\sqrt{R^2+1}}{(2/P)-1-R-\sqrt{R^2+1}}\right)}$$

$$= \frac{\frac{\sqrt{0.9788^2+1}}{0.9788-1} ln\left(\frac{1-0.3283}{1-0.3283\times0.9788}\right)}{ln\left(\frac{(2/0.3283)-1-0.9788+\sqrt{0.9788^2+1}}{(2/0.3283)-1-0.9788-\sqrt{0.9788^2+1}}\right)} = 0.9601$$

2.2 Estimation of the overall heat transfer coefficientof this shell and multipass tube heat exchanger:

Typically, a heat exchanger involves two flowing fluids separated by the tube's solid wall. Heat is first transferred from the hot fluid to the tube wall by convection, through the wall by conduction, and from the wall to the cold fluid again by convection.

The thermal resistance network associated with this heat transfer process involves two convection resistances and one conduction resistance, as shown in Figure III.7 The analysis is very similar to the previous study presented in Chap. 1. Here the subscripts i and o represent the inner and outer surfaces of the tube. For our heat exchanger configuration, the thermal resistance of the tube wall is:

$$R_{wall} = \frac{ln\left(\frac{D_o}{D_i}\right)}{2\pi\lambda L}$$

where λ is the thermal conductivity of the wall material and L is the length of the tube. Then the total thermal resistance becomes:

$$R = R_{total} = R_i + R_{wall} + R_o = \frac{1}{h_i A_i} + \frac{ln\left(\frac{D_o}{D_i}\right)}{2\pi\lambda L} + \frac{1}{h_o A_o}$$

The A_i is the area of the inner surface of the wall that separates the two fluids, and A_o is the area of the outer surface of the wall. In other words, Ai and A_o are surface areas of the separating wall wetted by the inner and the outer fluids, respectively.

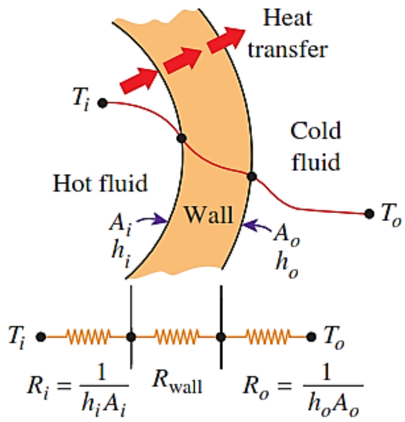

Figure III.7 Thermal resistance network associated with heat transfer in a shell and multipass tube heat exchanger.

In the analysis of heat exchangers, it is convenient to combine all the thermal resistances in the path of heat flow from the hot fluid to the cold one into a single resistance R and to express the rate of heat transfer between the two fluids as:

$$Q = \frac{\Delta T}{R} = UA\Delta T = U_i A_i \Delta T = U_o A_0 \Delta T$$

where A_s is the surface area and U is the overall heat transfer coefficient, whose unit is $W/m^2{\cdot}K$, which is identical to the unit of the ordinary convection coefficient h. Canceling ΔT, the above equation reduces to:

$$\frac{1}{UA_s} = \frac{1}{U_i A_i} = \frac{1}{U_o A_o} = R = \frac{1}{h_i A_i} + R_{wall} + \frac{1}{h_o A_o}$$

In fact, we have two overall heat transfer coefficients U_i and U_o for any heat exchanger. The reason is that every heat exchanger has two heat transfer surface areas A_i and A_o, which, in general, are not equal to each other, namely in the case of thick tubes.

In an attempt to estimate the overall coefficient of heat transfer inside the shell and multipass tube heat exchanger, we can proceed as follows:

The rate of heat transfer between the two fluids can be calculated, as follows:

- Case of oil-water shell and multipass tube heat exchanger with opposite inputs:

$$Q = C_h \left(T_{h,in} - T_{h,out}\right) = 294.4301(100 - 59.42) = 11.948kW$$

$$Q = F.U.A_s.\Delta T_{LM,CF}$$

Where:

$$\Delta T_{LM,CF}=\frac{\left(T_{h,in}-T_{c,out}\right)-\left(T_{h,out}-T_{c,in}\right)}{\ln\left(\frac{T_{h,in}-T_{c,out}}{T_{h,out}-T_{c,in}}\right)}=\frac{(100-35.56)-(59.42-15)}{\ln\left(\frac{100-35.56}{59.42-15}\right)}=53.81°C$$

the overall coefficient of heat transfer U_o, referred to the internal surface A_o as:

$$Q=F.U_0.A_0.\Delta T_{LM,CF}$$

$$\Rightarrow Q=F.U_o.\left[\left(n_t\pi D_{t,o}L_t\right)+\left((n-1)\pi\left(\frac{D_{arc,o}+D_{arc,in}}{4}\right).\pi.D_{t,o}\right)+\left(2\times0.3\times\pi D_{t,o}\right)\right].\Delta T_{LM,CF}$$

$$\Rightarrow U_o=\frac{Q}{F.\left[\left(n_t\pi D_{t,o}L_t\right)+\left((n-1)\pi\left(\frac{D_{arc,o}+D_{arc,in}}{4}\right).\pi.D_{t,o}\right)+\left(2\times0.3\times\pi D_{t,o}\right)\right].\Delta T_{LM,CF}}$$

$$U_o=\frac{11.948\times10^3}{0.9492\times\left[(11\times\pi\times0.044)+\left(10\pi^2\left(\frac{0.044+0.04}{4}\right)\times0.044\right)+(0.6\times\pi\times0.044)\right]\times53,81}$$

$$\Rightarrow U_o=138.0326(W/m^2.°C)$$

In a similar way, one can determine the overall coefficient of heat transfer U_i, referred to the internal surface A_i as:

$$\Rightarrow Q=F.U_i.A_i.\Delta T_{LM,CF}$$

$$\Rightarrow Q=F.U_i.\left[\left(n_t\pi D_{t,i}L_t\right)+\left((n-1)\pi\left(\frac{D_{arc,o}+D_{arc,in}}{4}\right).\pi.D_{t,i}\right)+\left(2\times0.3\times\pi D_{t,i}\right)\right].\Delta T_{LM,CF}$$

$$\Rightarrow U_i=\frac{Q}{F.\left[\left(n_t\pi D_{t,i}L_t\right)+\left((n-1)\pi\left(\frac{D_{arc,o}+D_{arc,in}}{4}\right).\pi.D_{t,i}\right)+\left(2\times0.3\times\pi D_{t,i}\right)\right].\Delta T_{LM,CF}}$$

$$U_i=\frac{11.948\times10^3}{0.9492\times\left[(11\times\pi\times0.04)+\left(10\pi^2\left(\frac{0.044+0.04}{4}\right)\times0.04\right)+(0.6\times\pi\times0.04)\right]\times53,81}$$

$$\Rightarrow U_i=151.8394(W/m^2.°C)$$

- Case of water-water shell and multipass tube heat exchanger with opposite inputs:

$$Q=C_h\left(T_{h,in}-T_{h,out}\right)=524.4017(100-72.09)=14.636kW$$

$$Q=F.U.A_s.\Delta T_{LM,CF}$$

Where:

$$\Delta T_{LM,CF} = \frac{(T_{h,in} - T_{c,out}) - (T_{h,out} - T_{c,in})}{\ln\left(\frac{(T_{h,in}-T_{c,out})}{(T_{h,out}-T_{c,in})}\right)} = \frac{(100 - 42.32) - (72.09 - 15)}{\ln\left(\frac{(100-42.32)}{(72.09-15)}\right)} = 57.38°C$$

the overall coefficient of heat transfer U_o, referred to the internal surface A_o as:

$$Q = F.U_0.A_0.\Delta T_{LM,CF}$$

$$\Rightarrow Q = F.U_o.\left[\left(n_t \pi D_{t,o} L_t\right) + \left((n-1)\pi\left(\frac{D_{arc,o} + D_{arc,in}}{4}\right).\pi.D_{t,o}\right) + \left(2\times 0.3\times \pi D_{t,o}\right)\right].\Delta T_{LM,CF}$$

$$\Rightarrow U_o = \frac{Q}{F.\left[\left(n_t \pi D_{t,o} L_t\right) + \left((n-1)\pi\left(\frac{D_{arc,o} + D_{arc,in}}{4}\right).\pi.D_{t,o}\right) + \left(2\times 0.3\times \pi D_{t,o}\right)\right].\Delta T_{LM,CF}}$$

$$= \frac{14.636 \times 10^3}{0.9601\left[(11 \times \pi \times 0.044) + \left(10\pi^2\left(\frac{0.044+0.04}{4}\right) \times 0.44\right) + (0.6 \times \pi \times 0.044)\right] \times 57.38}$$

$$\Rightarrow U_o = 172.4465\left(\frac{W}{m^2 \cdot °C}\right)$$

In a similar way, one can determine the overall coefficient of heat transfer U_i, referred to the internal surface A_i as:

$$\Rightarrow Q = F.U_i.A_i.\Delta T_{LM,CF}$$

$$\Rightarrow Q = F.U_i.\left[\left(n_t \pi D_{t,i} L_t\right) + \left((n-1)\pi\left(\frac{D_{arc,o} + D_{arc,in}}{4}\right).\pi.D_{t,i}\right) + \left(2\times 0.3\times \pi D_{t,i}\right)\right].\Delta T_{LM,CF}$$

$$\Rightarrow U_i = \frac{Q}{F.\left[\left(n_t \pi D_{t,i} L_t\right) + \left((n-1)\pi\left(\frac{D_{arc,o} + D_{arc,in}}{4}\right).\pi.D_{t,i}\right) + \left(2\times 0.3\times \pi D_{t,i}\right)\right].\Delta T_{LM,CF}}$$

$$= \frac{14.636 \times 10^3}{0.9601\left[(11 \times \pi \times 0.04) + \left(10\pi^2\left(\frac{0.044+0.04}{4}\right) \times 0.04\right) + (0.6 \times \pi \times 0.04)\right] \times 57.38}$$

$$\Rightarrow U_i = 156.7695\left(\frac{W}{m^2 \cdot °C}\right)$$

Note that $U_iA_i = U_oA_o$, but $U_i \neq U_o$ unless $A_i = A_o$. Therefore, the overall heat transfer coefficient U of a heat exchanger is meaningless unless the area on which it is based is specified. This is especially the case when one side of the tube wall is finned and the other side is not, since the surface area of the finned side is several times bigger than that of the unfinned side.

- we have in the case of water-water shell and multipass tube heat exchanger the coefficient of heat transfer h_o
  U_o=172.4465 W/m^2. °C , U_i =156.7695 W/m^2.°C , h_i =732.71 W/m^2.°C , A_i=1.5406 m^2 , A_o=1.9647 m^2 , λ=387.6 W/m^2.°C

$$U_i \cdot A_i = \frac{1}{\frac{1}{h_i A_i} + \frac{\ln\left(\frac{d_o}{d_i}\right)}{2\pi\lambda L} + \frac{1}{h_o A_o}} \Rightarrow h_o = \frac{1}{A_o\left(\frac{1}{U_i A_i} - \frac{1}{h_i A_i} - \frac{\ln\left(\frac{d_o}{d_i}\right)}{2\pi\lambda L}\right)}$$

$$h_o = \frac{1}{1.96 \times \left(\frac{1}{1.54\times156.75} - \frac{1}{732.71\times1.54} - \frac{\ln\left(\frac{0.044}{0.04}\right)}{2\times\pi\times387.6\times13.8}\right)} = 156.52\left(\frac{W}{m^2\cdot°C}\right)$$

- in the case oil-water shell and multipass tube heat exchanger the coefficient of heat transfer h_o.
  U_o=138.0326 W/m^2.°C , U_i =151.8394 W/m^2.°C , h_i =591.72 W/m^2.°C , A_i=1.5406 m^2 , A_o=1.9647 m^2 , λ=387.6 W/m^2.°C

$$U_i \cdot A_i = \frac{1}{\frac{1}{h_i A_i} + \frac{\ln\left(\frac{d_o}{d_i}\right)}{2\pi\lambda L} + \frac{1}{h_o A_o}} \Rightarrow h_o = \frac{1}{A_o\left(\frac{1}{U_i A_i} - \frac{1}{h_i A_i} - \frac{\ln\left(\frac{d_o}{d_i}\right)}{2\pi\lambda L}\right)}$$

$$h_o = \frac{1}{1.96 \times \left(\frac{1}{1.54\times151.83} - \frac{1}{591.72\times1.54} - \frac{\ln\left(\frac{0.044}{0.04}\right)}{2\times\pi\times387.6\times13.8}\right)} = 160.22\left(\frac{W}{m^2\cdot°C}\right)$$

2.3. Estimation of the effectiveness of this shell and multipass tube heat exchanger:

The effectiveness of a heat exchanger is defined as the ratio of the actual heat transfer rate exchanged and the maximum possible heat transfer rate.

$$\varepsilon = \frac{Q}{Q_{max}} = \frac{\text{Actual heat transfer rate}}{\text{maximum possible heat transfer rate}}$$

The actual heat transfer rate in a heat exchanger can be determined from an energy balance on the hot or cold fluids and can be expressed as:

$$Q = C_h\left(T_{h,in} - T_{h,out}\right) = C_c\left(T_{c,out} - T_{c,in}\right)$$

where $C_c = m_c \times Cp_c$ and $C_h = m_h \times Cp_h$ are the heat capacity rates of the cold and hot fluids, respectively.

To determine the maximum possible heat transfer rate in a heat exchanger, we first recognize that the maximum temperature difference in a heat exchanger is the difference between the inlet temperatures of the hot and cold fluids. That is,

$$\Delta T_{\max} = T_{h,in} - T_{c,in}$$

The heat transfer in a heat exchanger will reach its maximum value when:

- The cold fluid is heated to the inlet temperature of the hot fluid
- The hot fluid is cooled to the inlet temperature of the cold fluid.

These two limiting conditions will not be reached simultaneously unless the heat capacity rates of the hot and cold fluids are identical (i.e., $C_c = C_h$). When $C_c \not\approx C_h$, which is usually the case, the fluid with the smaller heat capacity rate will experience a larger temperature change, and thus it will be the first to experience the maximum temperature, at which point the heat transfer will come to a halt. Therefore, the maximum possible heat transfer rate in a heat exchanger is:

$$Q_{max} = C_{min}\left(T_{h,in} - T_{c,in}\right)$$

where C_{min} is the smaller of C_h and C_c.

- Case of oil-water shell and multipass tube heat exchanger with opposite inputs:

$$\varepsilon = \frac{Q}{Q_{max}} = \frac{C_h\left(T_{h,in} - T_{h,out}\right)}{\left(C_{min} = C_h\right)\left(T_{h,in} - T_{c,in}\right)} = \frac{\left(T_{h,in} - T_{h,out}\right)}{\left(T_{h,in} - T_{c,in}\right)} = \frac{\left(100 - 59.42\right)}{\left(100 - 15\right)} = 0.4774$$

- Case of water-water shell and multipass tube heat exchanger with opposite inputs:

$$\varepsilon = \frac{Q}{Q_{max}} = \frac{C_h\left(T_{h,in} - T_{h,out}\right)}{\left(C_{min} = C_h\right)\left(T_{h,in} - T_{c,in}\right)} = \frac{\left(T_{h,in} - T_{h,out}\right)}{\left(T_{h,in} - T_{c,in}\right)} = \frac{(100 - 72.09)}{(100 - 15)} = 0.3283$$

	T_{cs} (°C)	T_{hs} (°C)	U_i $\left(\frac{W}{m^2 \cdot °C}\right)$	U_o $\left(\frac{W}{m^2 \cdot °C}\right)$	F	$F\Delta T_{LM}$ (°C)	Q (kW)	ε	h_i $\left(\frac{W}{m^2 \cdot °C}\right)$	h_o $\left(\frac{W}{m^2 \cdot °C}\right)$
Oil-water	35.56	59.4	151.83	138.03	0.94	51.07	11.94	0.47	732.71	160.22
Water-water	42.32	72.09	179.416	156.76	0.96	55.09	14.63	0.32	591.72	156.52

TableIII.1: The final results obtained from both the outputs of the CFD software and the numerical calculation.

3. Conclusion and perspectives:

The primary objective of this study was to use a comprehensive 3D predictive numerical simulation to analyze the performance of a shell and multipass tube heat exchanger. This type of heat exchanger is widely used across various scales, from household to industrial applications. The study focused on the impact of different parameters on the thermal efficiency of the heat exchanger, with particular attention paid to variation in heat transfer fluids and the arrangement of inlet and outlet ports. The outcomes of the investigation were presented in terms of the temperature field, dynamic field, and thermal performance calculations.

In light of the results of our numerical analysis and investigations, we found that the oil-water configuration was more thermally efficient than the water-water configuration, due to the lower heat capacity rate of oil. Furthermore, we concluded that the efficiency of each type of configuration used in shell and multipass tube heat exchangers depends on the specific process requirements. For instance, the water-water configuration may be suitable for heating a cold fluid, while the oil-water configuration may be better for cooling a hot fluid. Ultimately, the choice of configuration should be based on the system's particular needs and desired outcomes, taking into account factors such as temperature differentials and fluid properties.

It is essential to note that this preliminary study is by no means completed, as heat exchangers have diverse applications with specific requirements. For example, our study only explored the effects of keeping the nature of the cold liquid which is water in each case. However, further investigations can be conducted by reversing the water with oil or another liquid or changing both fluids' properties to evaluate their impact on thermal and dynamic parameters. Additionally, there are various geometries and setups to try, and the possibilities for optimizing heat exchangers and searching for better operational conditions are endless.

In conclusion, we hope that our work has met your expectations and contributed, even in a small way, to scientific research. We also hope that this experience has opened our eyes to higher academic and professional opportunities and that it can serve as a helpful resource for other students conducting similar studies.

REFERENCES:

[1] Fundamentals of Heat Exchanger Design , Ramesh K. Shah, Dušan P. SekulićFirst, 1st Edition (2003) John Wiley & Sons, USA.

[2] Heat Exchanger Design Handbook, KuppanThulukkanam, 2nd Edition (2013), crc press, new York, USA.

[4] Heat Exchanger, selection, rating, and thermal design, 3rd Edition 2012, S adikKakac, Hongtanliu, AnchasaPramuanjaroenkij, crc press, new York, USA.

[5] Heat and Mass Transfer Fundamentals and Applications, Yunus A. Çengel, Afshin J. Ghajar, 5th Edition (2015), McGraw-Hill Education, USA.

[6] Chen, S. S., and Jendrzejczyk, J. A., Stability of tube arrays in crossflow, Nuclear Eng. Design, 75(3), 351-374 (1983)

[7] Transfert Thermique, Ana-Maria Bianchi, Yves Fautrelle, Jacqueline Etay, Presses Polytechniques et Universitaires Romandes (PPUR) 2004, France.

[8] Introduction to thermodynamics and heat transfer Yunus a. cengel. 2008, McGraw-Hill, USA

[9] Initiation aux transferts thermiques, Jean-François Sacadura, Jean-Paul Barrand, 1993, Lavoisier, Paris

[10] ANSYS Fluent Users Guide.pdf.

[11] https://mechanicalengineering.blog.

[12] https://savree.com/en/encyclopedia.

[13] https://www.cadfem-an.com/ansys.html.